Macromolecules

ARTICLE

pubs.acs.org/Macromolecules

Facile Synthesis of Hyperbranched and Star-Shaped Polymers by RAFT Polymerization Based on a Polymerizable Trithiocarbonate

Chengbo Zhang,[†] Yuan Zhou,[†] Qiang Liu,[†] Shixian Li,[†] Sébastien Perrier,[‡] and Youliang Zhao*[,†]

[†]Key Lab of Organic Synthesis of Jiangsu Province, College of Chemistry, Chemical Engineering and Materials Science, Soochow University, Suzhou 215123, China

[‡]Key Centre for Polymers & Colloids, School of Chemistry, The University of Sydney, NSW 2006, Australia

Supporting Information

ABSTRACT: Facile synthesis of hyperbranched and star polymers on the basis of *S*-(4-vinyl)benzyl *S*′-propyltrithiocarbonate (VBPT) was described. RAFT copolymerization of VBPT with vinyl monomers such as methyl methacrylates (MMA), styrene (St), methyl acrylate (MA), and *tert*-butyl acrylate (*t*BA) afforded hyperbranched copolymers with variable branch length and degree of branching. Hyperbranched copolymers obtained at a low feed ratio of vinyl monomers to VBPT usually possessed repeat units per branch higher than the expected values due to the presence of VBPT unit with pendant trithiocarbonate group and side reactions resulting in partial loss of CTA functionality. RAFT copolymerization at various feed ratios afforded poly(VBPT-*co*-MA) branched copolymers with weight-average CTA functionality up to 107 or more, which were further used to generate star PSt and P*t*BA with adjustable molecular weight and variable polydispersity (1.12 < PDI < 1.88). The approach based on two successive RAFT processes is general and versatile to synthesize multiarm star polymers with controllable arm length. The resultant polymers were characterized by ^{1}H NMR, GPC-MALLS, DSC, and TGA. The intrinsic viscosities of branched and star-shaped polymers were lower than those of their linear analogues with the same molecular weights; both Mark−Houwink−Sakurada exponent and contractor factor of branched copolymers were observed to increase with decreasing degree of branching, thus confirming a branching nature. The single glass transition temperature in DSC traces indicated branched copolymers obtained at various feed ratios had good compatibility.

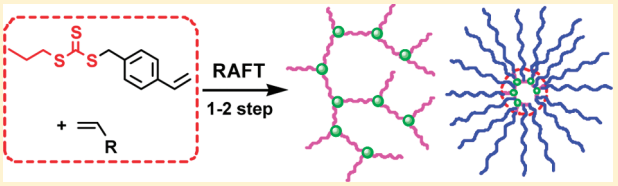

INTRODUCTION

Synthesis and properties of functional branched and star polymers have attracted much attention since these polymers usually possess unique physicochemical properties and wide applications originating from a large number of chain ends per molecule and their branched chain architectures.[1−29] Generally, hyperbranched polymers can be synthesized by step-growth polymerization via polycondensation or addition polymerization of multifunctional monomers,[3,4,30−32] copolymerization of conventional monomers via self-condensing vinyl polymerization (SCVP),[33−37] or copolymerization of vinyl monomers in the presence of multifunctional vinyl comonomers.[38,39] "Living"/controlled radical polymerization approaches such as iniferter-mediated polymerization,[40] nitroxide-mediated polymerization,[41] atom transfer radical polymerization,[42−44] and reversible addition−fragmentation chain transfer (RAFT) polymerization[45−53] have been efficiently used to synthesize a variety of hyperbranched and star polymers with controlled compositions and variable functionality. Among them, RAFT polymerization is a facile and versatile approach to synthesize hyperbranched and star polymers due to its many advantages such as relatively mild reactions, wide range of monomers, tolerance of various functionalities, and lack of metal catalyst. A range of hyperbranched polymers have been achieved by RAFT polymerization in the presence of divinyl comonomers,[38,39] from a polymer backbone with pendant xanthate groups,[54] or with AB* styryl or acryloyl chain transfer agents.[55−58] Until now, the types of hyperbranched polymers obtained via RAFT process were relatively limited, and the feed ratio of vinyl monomer to chain transfer agent was usually higher than 10. In particular, the copolymerization behavior of conventional monomer with polymerizable RAFT agent has not been thoroughly investigated. It is therefore of great interest to study in depth the dependence of copolymer composition and degree of branching (DB) of hyperbranched copolymers on reaction conditions during RAFT polymerization.

Star polymers, on the other hand, have been well-studied. They can be synthesized by approaches such as "arm first",[59−63] "core first",[64−67] and their combination.[68−71] The arm first approach involves the synthesis of prefabricated arms, usually through "living"/controlled polymerization, followed by reaction with a multifunctional core reagent, which is easily performed and can also afford target star polymers with low polydispersity. The potential drawback of arm first method is that the arm

Received: October 31, 2010
Revised: January 22, 2011
Published: March 11, 2011

number is usually uncertain, the chemical structure of branched core is very complex, and the remaining linear chains are necessary to be removed by fractional precipitation in some cases. The core first approach involves the use of multifunctional initiator or chain transfer agent (CTA), and the arm numbers in star polymers can be determined by the functionality on the initiator/CTA, by which a series of well-defined star polymers with exact arm number up to 24 or more have been achieved.[11−13,72−77] The major drawback of the core first method lies in complex multistep syntheses of multifunctional compounds and possible defects in macromolecular architecture resulting from partly unreacted sites on functional cores since the reaction was closely related to the nature of core reagents and initiation conditions.[9−13,77] Thus, there is a need to overcome the shortcomings of these methods.

For synthesis of star polymer via controlled radical polymerization, star−star coupling is usually observed if the functional initiator is very compact,[53] and we have demonstrated this disadvantage can be partly addressed by using multifunctional poly(aryl ether) dendrimer initiators with large molecular size and rigidity.[11−13] However, the synthesis of dendrimers usually requires multistep syntheses and drastic purifications between each step, making it a costly and time-consuming process. This disadvantage is hopefully addressed by RAFT copolymerization of a polymerizable CTA with conventional vinyl monomers. So far, such reactions were only used to prepare hyperbranched polymers,[55−58] and reports on synthesis of multifunctional initiators/CTAs by RAFT process to further generate star-shaped polymers are very scarce.[20] More recently, Kakwere et al. described a facile route to star-shaped copolymers by combination of RAFT and ring-opening polymerization (ROP), in which the multifunctional initiators were synthesized by RAFT copolymerization of ethyl acrylate with hydroxyethyl acrylate, and the subsequent ROP of L-lactide could afford miktoarm stars with controlled molecular weight and polydispersity ranging between 1.3 and 1.9.[20]

In this study, a modified method based on two successive RAFT processes was developed to synthesize star-shaped polymers. Branched multifunctional CTAs with relatively low polydispersity and variable CTA functionality were obtained by RAFT copolymerization of polymerizable RAFT agent *S*-(4-vinyl)benzyl *S*′-propyltrithiocarbonate (VBPT) with conventional vinyl monomers such as methyl acrylate (MA), methyl methacrylate (MMA), styrene (St), or *tert*-butyl acrylate (*t*BA), and star-shaped polymers with a branched core and variable arm length and polydispersity were then synthesized by a subsequent RAFT polymerization. The branched multifunctional cores obtained via RAFT copolymerization possess relatively large molecular size; thus, the probability for star−star coupling may be further lowered during the subsequent RAFT process to generate star polymers. In addition, the C═C double bond of a polymerizable RAFT agent has a different reactivity from that of other vinyl monomers; therefore, RAFT copolymerization using various comonomer feed ratios enables the synthesis of branched copolymers with different compositions and sequential structures and various CTA functionality.

EXPERIMENTAL SECTION

Materials. All solvents, monomers, and other chemicals were purchased from Alfa Aesar unless otherwise stated. 4-Vinylbenzyl chloride (90%), sodium methoxide (95%), and 1-propanethiol (99%) were purchased from Sigma-Aldrich. Methyl acrylate (MA, 99%), *tert*-butyl acrylate (*t*BA, 98%), methyl methacrylate (MMA, 99%), and styrene (St, 99%) were passed through a basic alumina (Brockmann I) column to remove the inhibitor before use. 2,2′-Azobis(isobutyronitrile) (AIBN) was recrystallized twice from ethanol. Other chemicals were of analytical grade and used as received.

Synthesis of VBPT. To a stirred solution of 1-propanethiol (99%, 15.4 g, 0.200 mol) in 160 mL of anhydrous methanol was slowly added a solution of sodium methoxide (95%, 11.5 g, 0.202 mol) in 200 mL of methanol under nitrogen. CS_2 (19.0 g, 0.250 mol) was added dropwise to the solution after 2 h, and the mixture was further stirred at ambient temperature for 5 h. To the yellow solution was slowly added 4-vinylbenzyl chloride (90%, 37.2 g, 0.219 mol), and the mixture was stirred overnight under nitrogen. The residue was partitioned between water and dichloromethane, and the aqueous layer was extracted twice with dichloromethane. The combined extracts were dried over $MgSO_4$. The crude product was purified by flash column chromatography eluting with hexane, and VBPT (46.6 g, 86.8% yield) was isolated as yellow viscous oil. ^{1}H NMR ($CDCl_3$): δ 7.34 and 7.30 (ABq, *J*8, 4H, Ar*H*), 6.69 and 6.67 (ABq, *J*7.2, 1H, C*H*), 5.75 (d, *J*17.6, 1H, CH_2), 5.26 (d, *J*11.2, 1H, CH_2), 4.59 (s, 2H, ArCH_2), 3.35 (t, *J*7.2, 2H, SCH_2), 1.74 (m, 2H, CH_3CH_2), 1.02 (t, *J*7.2, 3H, CH_3CH_2). ^{13}C NMR ($CDCl_3$): δ 223.6, 137.0, 136.2, 134.6, 129.4, 126.5, 114.2, 44.1, 38.9, 21.6, 13.5. FTIR (cm^{-1}): 3086, 2963, 2927, 2870, 1629, 1566, 1510, 1457, 1405, 1379, 1337, 1288, 1238, 1198, 1082, 1063, 1047, 988, 908, 816, 733, 706, 683. Anal. Calcd for $C_{13}H_{16}S_3$: C, 58.16%; H, 6.01%; S, 35.83%. Found: C, 58.15%; H, 6.03%; S, 35.77%.

Synthesis of Hyperbranched Copolymers by RAFT Copolymerization of VBPT with Vinyl Monomers. RAFT copolymerization was conducted in toluene using AIBN as the primary radical source and VBPT as the polymerizable CTA. In a typical polymerization (run 3 of Table 1), MA (0.431 g, 5.0 mmol), VBPT (2.685 g, 10.0 mmol), and AIBN (0.164 g, 1.0 mmol) were added to a glass tube with a magnetic stirring bar, and toluene was added until the total volume was 5.0 mL. The tube was sealed with a rubber septum, and the contents were flushed with nitrogen for 10 min. The tube was subsequently immersed into an oil bath preheated to 60 °C. After 96 h, the polymerization was quenched by putting the tube into an ice−water bath. The homogeneous solution (about 0.1 mL) was directly diluted with $CDCl_3$ and subjected to NMR analysis, and the monomer conversions were determined to be 99.5% (for VBPT) and 100% (for MA) by comparing the integrated areas of characteristic signals of monomer and polymer. After precipitating into a large amount of cold hexane thrice, 2.95 g of poly(VBPT-*co*-MA) hyperbranched copolymer was isolated, and its molecular weight and polydispersity were obtained by GPC-MALLS: M_n = 11 800, PDI = 3.09. Other polymers were synthesized according to a similar approach and obtained by precipitation into cold hexane or methanol (for branched poly(VBPT-*co*-St) and poly(VBPT-*co*-MMA)) or methanol/water mixtures (for branched poly(VBPT-*co*-*t*BA)). The monomer conversions (*C*%) were determined by ^{1}H NMR by comparing the integrated areas of characteristic signals of monomer and polymer using the following equations: $C_{VBPT} = 1-3I_{5.26}/I_{1.02}$, $C_{MA} = 1-3I_{6.14}/I_{3.6-3.9}$, $C_{MMA} = I_{3.59}/I_{3.5-3.8}$, and $C_{tBA} = 1-9I_{5.98}/I_{1.44}$, where I_{a-b} means the integrated areas from *a* to *b* ppm in ^{1}H NMR spectra of mixture obtained by RAFT polymerization. For RAFT copolymerization of VBPT with St, it was quite difficult to directly determine monomer conversions by ^{1}H NMR due to significant overlapping signals; thus, the combination of the gravimetric method and the ^{1}H NMR method was used to work out monomer conversions. The molar ratio of reacted VBPT to St unit was calculated by NMR analysis of isolated branched copolymer (F_{VBPT}:$F_{St} = 5I_{1.02}/(3I_{6.2-7.3} - 4I_{1.02})$, where F_{VBPT} is the molar fraction of VBPT participated in the copolymerization and F_{St} is the molar fraction of St unit in the branched copolymer), and monomer conversions were then deduced on the basis of the total weight conversion obtained by gravimetry.

Table 1. Results for RAFT Copolymerization of VBPT (M_1) with MA (M_2) Under Various Conditions[a]

run	x	t (h)	C_{M1} (%)[b]	C_{M2} (%)[b]	M_n[c]	PDI[c]	RB(th)[d]	RB[e]	DB[e]	P_1 (%)[f]	P_2 (%)[f]	F[g]	f_{CTA}[h]
1	0.2	96	95.4	100	6 120	2.38	1.21	5.30	0.189	86.8	2.39	45.3	0.889
2	0.4	96	99.8	100	9 200	2.72	1.40	6.29	0.159	86.2	3.06	74.6	0.902
3	0.5	96	99.5	100	11 800	3.09	1.50	6.32	0.158	83.6	5.92	107	0.912
4	1	96	96.3	100	12 500	2.58	2.04	6.48	0.154	75.4	12.8	82.0	0.909
5	2.5	96	97.5	100	10 800	2.42	3.56	6.42	0.156	50.8	39.7	46.8	0.875
6	5	21	92.7	66.3	11 600	2.07	4.58	7.63	0.131	41.5	56.8	40.2	0.964
7	5	96	98.3	100	17 600	2.60	6.09	8.55	0.117	31.5	60.9	59.3	0.914
8	10	21	96.1	53.5	9 540	1.86	6.57	9.03	0.111	29.1	67.6	22.3	0.937
9	10	96	99.2	100	18 700	2.02	11.1	13.2	0.0758	18.8	78.5	28.8	0.866
10	20	21	97.8	72.7	9 860	2.04	15.9	17.2	0.0581	8.33	84.4	11.8	0.906
11	20	96	99.7	100	16 200	2.18	21.1	22.3	0.0448	6.52	87.5	14.7	0.831
12	50	10	86.5	42.4	7 380	1.56	25.5	26.4	0.0379	3.51	91.2	4.62	0.953
13	50	96	100	100	19 000	2.02	51.0	51.3	0.0195	0.65	93.1	6.36	0.757
14	100	5	90.2	36.7	8 530	1.61	41.7	44.6	0.0224	6.71	85.9	3.58	0.981
15	100	96	100	100	30 700	2.43	101	101	0.0099	0	99.2	6.29	0.749
16	5	24	53.3	18.8	4 080	1.16	2.76	5.50	0.182	52.1	45.4	10.8	0.955
17	10	24	77.2	25.2	5 350	1.22	4.26	7.39	0.135	45.6	51.8	11.0	0.928
18	20	24	92.1	48.5	8 160	1.36	11.5	12.5	0.080	8.37	87.2	8.52	0.901
19	50	24	99.5	82.2	12 300	1.95	42.3	43.0	0.0233	1.82	91.3	5.41	0.862

[a] Polymerization conditions: $[MA]_0$:$[VBPT]_0$:$[AIBN]_0 = x$:1:0.1, $[MA]_0 + [VBPT]_0 = 3.0$ mol/L (runs 1−15), or $[AIBN]_0 = 3.0$ mmol/L (runs 16−19), in toluene at 60 °C. [b] VBPT (C_{M1}) and MA (C_{M2}) conversions determined by ^{1}H NMR. The associated error in measuring integrated NMR signals for all polymer samples was estimated to be ±5%. [c] Molecular weight and polydispersity determined by GPC-MALLS. [d] Theoretical repeat units per branch calculated by equation $RB(th) = ([MA]_0 \times C_{M2})/([VBPT]_0 \times C_{M1}) + 1$. [e] Determined by ^{1}H NMR, herein $RB = (I_{3.65}/3 + I_{6.6-7.3}/4)/(I_{6.6-7.3}/4 - I_{4.56}/2)$ where I means peak area at various chemical shifts, and DB = 1/RB. [f] Proportions of terminal trithiocarbonate functionality connecting with benzyl group (P_1) or MA unit (P_2) in branched copolymers, $P_1 = I_{4.56}/2(I_{4.87} + I_{4.56}/2 + I_{4.18})$, and $P_2 = I_{4.87}/(I_{4.87} + I_{4.56}/2 + I_{4.18})$. [g] Weight-average CTA functionality per branched copolymer, $F = M_w(LS) \times (I_{4.87} + I_{4.56}/2 + I_{4.18})/(MW_{VBPT} \times I_{6.6-7.3}/4 + MW_{MA} \times I_{3.65}/3)$. [h] Molar ratio of residual trithiocarbonate functionality in branched copolymer to VBPT participated in RAFT copolymerization, $f_{CTA} = 4(I_{4.87} + I_{4.56}/2 + I_{4.18})/I_{6.6-7.3}$.

Poly(VBPT-*co*-MA) branched copolymer: ^{1}H NMR ($CDCl_3$): δ 6.6−7.3 (ArH, VBPT unit), 4.87 ($CH_3COOCHS$, terminal MA unit), 4.56 (CH(Ar)CH_2S, VBPT unit), 4.18 (CH_2(Ar)CHS, styryl unit originated from reacted VBPT), 3.65 ($COOCH_3$, MA unit), 3.47, 3.36, and 2.99 ($CH_3CH_2CH_2$S, terminal trithiocarbonate functionality), 1.1−2.8 (CH_2 and CH, VBPT and MA units), 1.02 ($CH_3CH_2CH_2$S, terminal trithiocarbonate functionality). FT-IR (KBr, cm^{-1}): 3048, 3020, 2958, 2925, 2869, 1732, 1640, 1510, 1422, 1378, 1236, 1194, 1157, 1081, 1058, 1041, 876, 803, 704, 675.

Poly(VBPT-*co*-MMA) branched copolymer: ^{1}H NMR ($CDCl_3$): δ 6.6−7.3 (ArH, VBPT unit), 4.56 (CH(Ar)CH_2S, VBPT unit), 4.18 (CH_2(Ar)CHS, styryl unit originated from reacted VBPT), 3.60 ($COOCH_3$, MMA unit), 3.36, 3.27, and 2.99 ($CH_3CH_2CH_2$S, terminal trithiocarbonate functionality), 2.87 ($CH_2C(CH_3)(COOCH_3)$S, terminal MMA unit), 0.4−2.6 (CH_3, CH_2 and CH, VBPT and MA units). FT-IR (KBr, cm^{-1}): 3050, 3020, 2956, 2928, 2870, 1728, 1639, 1510, 1451, 1379, 1287, 1237, 1194, 1131, 1082, 1061, 1044, 987, 876, 805, 704, 676.

Poly(VBPT-*co*-St) branched copolymer: ^{1}H NMR ($CDCl_3$): δ 6.6−7.3 (PhH and ArH, VBPT and St units), 4.6−5.1 (PhCH(CH_2)S, terminal St unit), 4.56 (CH(Ar)CH_2S, VBPT unit), 4.18 (CH_2(Ar)CHS, styryl unit originated from reacted VBPT), 3.36, 3.24, and 2.99 ($CH_3CH_2CH_2$S, terminal trithiocarbonate functionality), 1.1−2.8 (CH_2 and CH, VBPT and St units), 1.02 ($CH_3CH_2CH_2$S, terminal trithiocarbonate functionality). FT-IR (KBr, cm^{-1}): 3055, 3023, 2960, 2920, 2852, 1640, 1509, 1492, 1451, 1419, 1287, 1236, 1194, 1061, 1043, 876, 807, 759, 698.

Poly(VBPT-*co*-*t*BA) branched copolymer: ^{1}H NMR ($CDCl_3$): δ 6.6−7.3 (ArH, VBPT unit), 4.75 (*t*BuCOOCHS, terminal *t*BA unit), 4.58 (CH(Ar)CH_2S, VBPT unit), 4.20 (CH_2(Ar)CHS, styryl unit originated from reacted VBPT), 3.36, 3.27, and 2.99 ($CH_3CH_2CH_2$S, terminal trithiocarbonate functionality), 1.1−2.8 (CH_3, CH_2 and CH, VBPT and *t*BA units), 1.02 ($CH_3CH_2CH_2$S, terminal trithiocarbonate functionality). FT-IR (KBr, cm^{-1}): 3048, 3002, 2963, 2926, 2870, 1722, 1642, 1609, 1510, 1453, 1421, 1366, 1252, 1144, 1041, 871, 842, 806, 752, 708.

Conventional Free Radical Polymerization of Vinyl Monomers and VBPT Polymerization via SCVP. MA (0.861 g, 10 mmol), AIBN (16.4 mg, 0.1 mmol), and toluene (2.4 mL) were placed in the glass tube equipped with a magnetic stirrer. The mixture was flushed with nitrogen for 10 min and polymerized at 60 °C for 6 h. The polymer was precipitated in hexane thrice and dried under reduced pressure at 40 °C until constant weight. Other linear polymers were synthesized according to similar conditions.

VBPT (1.34 g, 5 mmol), AIBN (8.2 mg, 0.05 mmol), and toluene (0.35 mL) were placed in the reactor equipped with a magnetic stirrer. The mixture was flushed with nitrogen for 10 min and polymerized at 60 °C for 24 h. The polymer was precipitated in hexane thrice. After drying under reduced pressure at 40 °C for 5 h, and hyperbranched PVBPT was obtained.

Synthesis of Star-Shaped Polymers with a Branched Core by RAFT Polymerization. In a typical polymerization (run 4 of Table 6), branched poly(VBPT-*co*-MA) (M_n = 3020, PDI = 1.35, F = 13.0, 46.7 mg, 0.15 mmol), St (1.56 g, 15 mmol), and AIBN (4.9 mg, 0.030 mmol) were added to a glass tube, and toluene was added until the total volume was 7.5 mL. The tube with a magnetic stirring bar was sealed with a rubber septum, and the contents were flushed with nitrogen for 15 min and polymerized at 60 °C for 10 h. The glass tube

dx.doi.org/10.1021/ma1024736 |*Macromolecules* 2011, 44, 2034–2049

Scheme 1. Synthesis of Branched Copolymers by RAFT Copolymerization of VBPT (M_1) with Vinyl Monomers (M_2) and Star-Shaped Polymers with a Branched Core via a Successive RAFT Process[a]

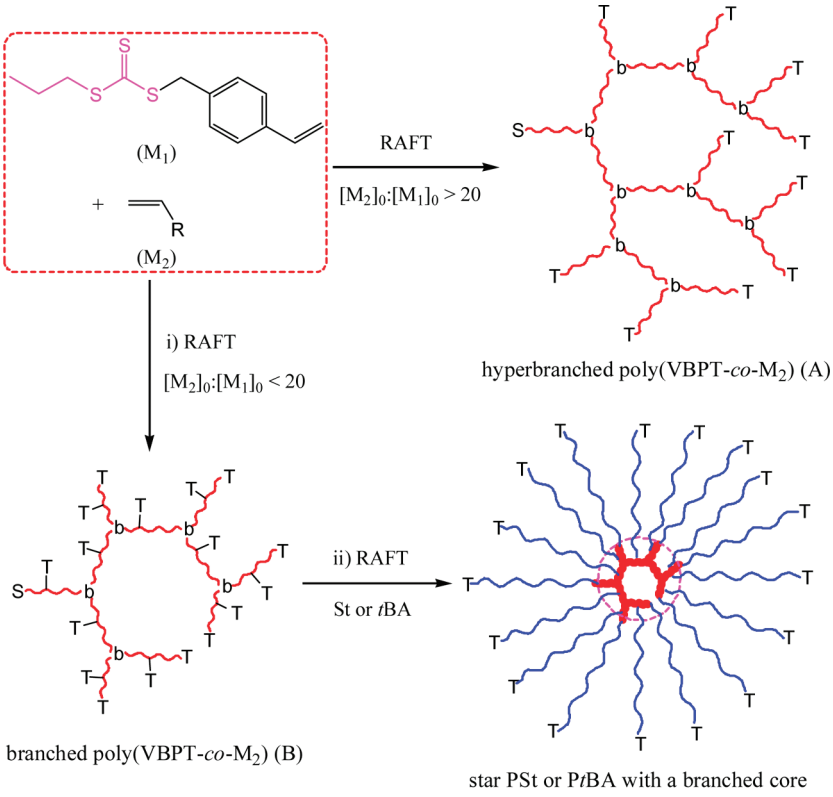

[a] M_2 = MMA, MA, *t*BA, St; S = styryl group; b = polymerized S group; T− = remaining unreacted CTA functionality inVBPT unit; T = terminal propyltrithiocarbonate group.

was removed and cooled to room temperature immediately. The star-shaped PSt with a branched core was recovered by precipitating its solution into cold methanol thrice, and the monomer conversion of 20.2% was determined by gravimetry. The molecular weight and polydispersity of star PSt as determined by GPC-MALLS were M_n = 36 200 and PDI = 1.88. Other star-shaped polymers were synthesized and recovered according to a similar approach using various macro-CTAs, and star P*t*BA was recovered by precipitation into mixtures of water and methanol.

Star PSt: ^{1}H NMR ($CDCl_3$): δ 6.2−7.5 (Ph*H* and Ar*H*, VBPT and St units), 5.12 (PhC*H*(CH_2)S, terminal St unit), 3.60 (CH_3OCO, MA unit), 3.25 ($CH_3CH_2CH_2$S, terminal trithiocarbonate functionality), 1.0−2.6 (CH_2 and C*H*, MA, VBPT and St units), 0.98 ($CH_3CH_2CH_2$S, terminal trithiocarbonate functionality). IR (KBr, cm^{-1}): 3081, 3059, 3025, 2921, 2849, 1943, 1870, 1802, 1735, 1648, 1600, 1582, 1544, 1493, 1452, 1373, 1154, 1067, 1027, 963, 906, 842, 842, 812, 756, 698.

Star P*t*BA: ^{1}H NMR ($CDCl_3$): δ 6.6−7.3 (ArH, VBPT unit), 4.68 (*t*BuCOOC*HS*, terminal *t*BA unit), 3.32 ($CH_3CH_2CH_2$S, terminal trithiocarbonate functionality), 1.1−2.8 (CH_3, CH_2 and C*H*, VBPT and *t*BA units), 1.01 ($CH_3CH_2CH_2$S, terminal trithiocarbonate functionality). IR (KBr, cm^{-1}): 3002, 2979, 2934, 2873, 1730, 1634, 1482, 1457, 1394, 1369, 1258, 1147, 1034, 910, 846, 752, 708.

Characterization. The gel permeation chromatography (GPC) systems were used to determine molecular weight, polydispersity (PDI), and solution viscosity of the obtained polymers. GPC was conducted in THF at 35 °C with a flow rate of 1 mL/min. Three TSK-GEL H-type columns (pore size 15, 30, and 200 Å, with molecular weight range of 100−1000, 300−20 000, and 5 000−400 000 g/mol, respectively) with 5 μm bead size were used. Detection consisted of a RI detector (Optilab rEX), a multiangle (14°−145°) laser light scattering (MALLS) detector (DAWN HELLOS) with the He−Ne light wavelength at 658.0 nm, and online viscosity detector (ViscoStar). The refractive index increment d*n*/d*c* for samples were measured off-line by Optilab rEX refractive index detector (λ = 658 nm) at 25 °C using a series of different concentration solutions. Data were collected and processed by use of ASTRA software from Wyatt Technology, and molecular weights were determined by the triple detection method. The intrinsic viscosity of the polymer solution in THF was measured using a viscosimetric detector connected to the GPC system at 35 °C. ^{1}H (400 MHz) and ^{13}C (100 MHz) NMR spectra were recorded on a Varian spectrometer at 25 °C using $CDCl_3$ as a solvent. Fourier transform infrared (FT-IR) spectra were recorded on a Perkin-Elmer 2000 spectrometer using KBr disks. Thermogravimetric analysis (TGA) and differential scanning calorimetric analysis (DSC) were performed using a SDT 2960 Simultaneous DSC-TGA of TA Instruments, and the heating rate was 10 °C/min under nitrogen.

RESULTS AND DISCUSSION

A polymerizable RAFT agent *S*-(4-vinyl)benzyl *S*′-propyltrithiocarbonate (VBPT) was synthesized and used to generate branched and star-shaped polymers via the RAFT process; VBPT acted as both chain transfer agent and core reagent to form branching unit during copolymerization. RAFT copolymerization between VBPT and vinyl monomers afforded hyperbranched

dx.doi.org/10.1021/ma1024736 |*Macromolecules* 2011, 44, 2034–2049

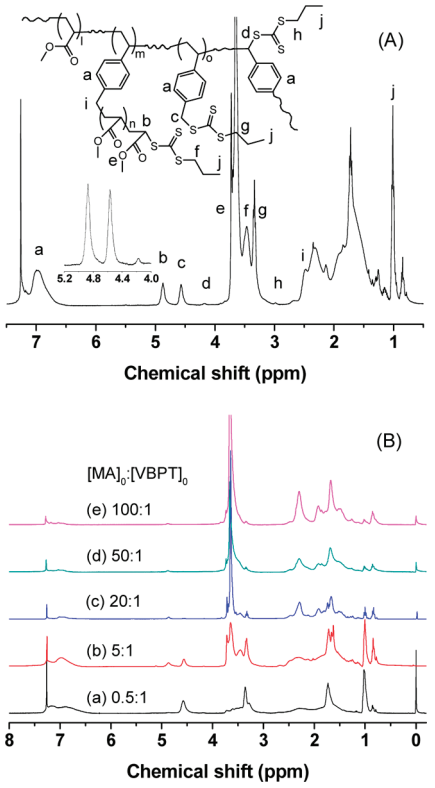

Figure 1. ^{1}H NMR spectra of poly(VBPT-*co*-MA) branched copolymers obtained by RAFT copolymerization: (A) $[MA]_0$:$[VBPT]_0$ = 10:1; (B) at various feed ratios. Samples were synthesized by runs 3, 6, 8, 10, 12, and 14 in Table 1.

copolymers with variable degree of branching (DB), polydispersity (PDI), and CTA functionality (F), and star-shaped polymers with a branched core were synthesized by a successive RAFT process (Scheme 1).

RAFT Copolymerization of VBPT with MA. Since the styryl group of VBPT has a different reactivity than that of other vinyl monomers, their RAFT copolymerization may afford branched copolymers with variable DB and F values. To investigate the effects of comonomer feed ratio, monomer and initiator concentrations, and reaction time on copolymerization, RAFT copolymerization of VBPT with MA was conducted in toluene at 60 °C, and the copolymerization results are listed in Table 1. The monomer conversions (C%) were determined by ^{1}H NMR by comparing the integrated areas of characteristic signals of monomer and polymer. In the ^{1}H NMR spectra of poly(VBPT-*co*-MA) branched copolymers, three types of groups connecting with the terminal trithiocarbonate functionality were observed. The signal of aromatic protons originating from VBPT participating in the copolymerization were noted at 6.6−7.3 ppm, and the signals of CHS in the terminal MA unit, CH_2S in the remaining VBPT unit with unreacted pendant trithiocarbonate moieties, and CHS in styryl unit originated from reacted VBPT appeared at 4.87, 4.56, and 4.18 ppm, respectively (Figure 1); thus, proportions of trithiocarbonate functionality connecting with benzyl group (P_1), terminal MA unit (P_2), and styryl unit (P_3, $P_1 + P_2 + P_3 = 1$) in hyperbranched copolymers could be determined. Furthermore, since side reactions such as termination and irreversible transfer could lead to a loss in CTA functionality, f_{CTA} was introduced to describe molar ratio of

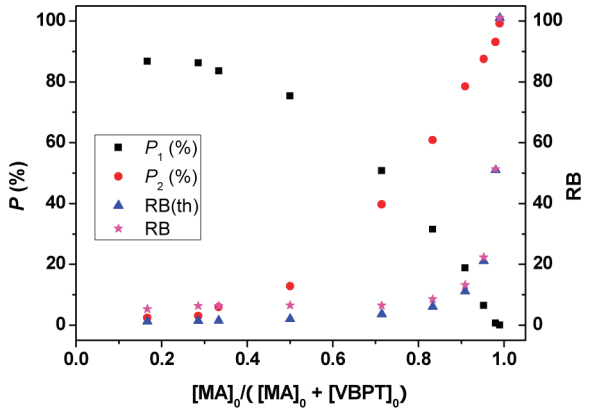

Figure 2. Dependence of P_1, P_2, and RB of branched poly(VBPT-*co*-MA) on comonomer feed ratio during RAFT copolymerization of VBPT with MA in toluene at 60 °C for 96 h.

residual trithiocarbonate functionality in branched copolymer to VBPT that participated in RAFT copolymerization, which could be determined by the equation $f_{CTA} = 4(I_{4.87} + I_{4.56}/2 + I_{4.18})/I_{6.6-7.3}$ (for branched poly(VBPT-*co*-MA)). As the proportion of remaining VBPT unit did not form the branching unit, the real repeat units per branch (RB) could be calculated by equation RB = RB(th)/(1 − $f_{CTA}P_1$). Since GPC analyses using RI detector usually underestimated the real molecular weight of star and hyperbranched polymers due to their different hydrodynamic volumes as compared with linear standard samples,[72−77] the resultant branched copolymers were subjected to GPC-MALLS measurements to determine accurate molecular weights. In Table 1, the weight-average CTA functionality per branched copolymer (F) was determined by combination of GPC-MALLS and NMR analysis by the equation $F = M_w(LS) \times (I_{4.87} + I_{4.56}/2 + I_{4.18})/(MW_{VBPT} \times I_{6.6-7.3}/4 + MW_{MA} \times I_{3.65}/3)$, where M_w(LS) is weight-average molecular weight determined by GPC-MALLS and MW_{VBPT} and MW_{MA} are molecular weights of VBPT and MA.

Effects of Comonomer Feed Ratio on RAFT Copolymerization. RAFT copolymerization of VBPT with MA was conducted in a wide range of feed ratio ($[MA]_0$:$[VBPT]_0 = x$), and the effects of comonomer feed ratio on copolymerization were investigated. When the total comonomer concentration was 3.0 mol/L, and x ranged from 0.2 to 100, the copolymerization results are listed in runs 1−15 of Table 1. For branched copolymers obtained by RAFT copolymerization using relatively low feed ratios (x = 0.2−2.5) for 96 h, number-average molecular weights (M_n) of branched copolymers ranged between 6120 and 12 500, polydispersity indices were varied from 2.38 to 3.09, and maximum weight-average molecular weight (M_w(LS) = 36 500) and CTA functionality (F = 107) were observed at a feed ratio of 0.5. For branched copolymers obtained by RAFT copolymerization using increased feed ratios (x = 5−100) for 96 h, the M_n values of branched copolymers ranged between 16 200 and 30 700, polydispersity indices were varied from 2.02 to 2.60, and the F value was gradually decreased from 59.3 to 6.29.

As a comparison, the dependence of P_1, P_2, and RB of branched poly(VBPT-*co*-MA) on comonomer feed ratio is shown in Figure 2. As $[MA]_0/([MA]_0 + [VBPT]_0)$ was raised from 0.167 to 0.99, P_1 was gradually decreased from 86.8% to 0, P_2 was gradually increased from 2.39% to 99.2%, and RB was varied between 5.3 and 101. When x was less than 20, RB was

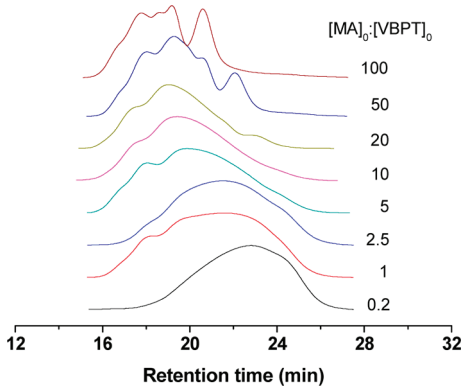

Figure 3. GPC traces of poly(VBPT-*co*-MA) branched copolymers obtained by RAFT copolymerization at various comonomer feed ratios for 96 h. See Table 1 for detailed reaction conditions.

usually significantly higher than theoretical value (RB(th)) assuming that any VBPT participated in RAFT copolymerization could form the branching unit. RB/RB(th) was about 4.4 (x = 0.2−0.5) and 3.2 (x = 1) and then gradually decreased from 1.8 (x = 2.5) to 1 (x = 100) with increasing x values. This phenomenon could be ascribed to the presence of unreacted trithiocarbonate functionality in VBPT unit and some side reactions such as termination and irreversible transfer. On one hand, the reactivity of MA was usually higher than that styryl group in VBPT unit, and VBPT and MA concentrations were comparable when x was less than 5, leading to formation of a large amount of VBPT unit with unreacted trithiocarbonate moieties in addition to branching unit (P_1 > 31.5%). During RAFT copolymerization, the branching unit could be formed only if both styryl group and trithiocarbonate functionality participated in RAFT copolymerization. When the styryl group was polymerized while part of trithiocarbonate functionality did not participate in RAFT polymerization due to lack of polymerizable monomers or low ability for RAFT process, the VBPT unit remained in the resultant branched copolymer, and this proportion of polymerized VBPT only played a role of conventional vinyl monomers other than branching agent. On the other hand, the probability of termination and irreversible transfer of chain radicals was significantly raised with extended reaction times due to lack of polymerizable monomers and increased viscosity of polymer solution. Molecular weights were significantly increased as coupling reactions between chain radicals happened, and part of the terminal CTA functionality in branched copolymer was also lost as chain radicals were subjected to disproportionation termination and chain transfer reactions to monomer, solvent, or polymeric chain. In Table 1, the f_{CTA} values of branched copolymers obtained at 96 h ranged between 0.749 and 0.914, and significant shoulders, tailings, or even multiple distributions appeared in GPC traces (Figure 3), suggesting partial loss of CTA functionality. Thus, both f_{CTA} and P_1 attributed to the increased RB values, and P_1 played a more important role at a low MA-to-VBPT ratio (x < 5).

For branched copolymers obtained at 96 h, the CTA functionality per branched copolymer was evaluated to be between 5.3 and 107. At a low feed ratio (x < 5), the F values of branched copolymers were higher than 45 even if the branched copolymer had relatively low molecular weight due to the presence of a large number of remaining VBPT units (P_1 > 31.5%). As $[MA]_0/([MA]_0 + [VBPT]_0)$ increased, P_1 and DB were observed to decrease, while P_2 and RB tended to increase. By careful inspection of the results in runs 6−15 of Table 1, it can be seen that RAFT copolymerization at longer time afforded branched copolymers with enhanced molecular weight, polydispersity, RB, P_2, and F values and lowered P_1, f_{CTA}, and DB, indicating these molecular parameters of branched copolymers were also strongly dependent on monomer conversions.

The above results revealed that the end-group compositions, degree of branching, and CTA functionality of branched copolymers could be efficiently adjusted by control over comonomer feed ratio and reaction time; thus, RAFT copolymerization of VBPT with MA at various feed ratios could afford poly(VBPT-*co*-MA) branched copolymers with a wide range of molecular weights, polydispersity indices, degrees of branching, and thiocarbonyl−thio functionalities in chain end and pendant group.

The aforementioned RAFT copolymerization afforded branched copolymers with polydispersity typically higher than 1.6. Theoretically, the polydispersity indices may be further lowered at slower polymerization rates or low conversions, which could be achieved by decreasing initiator or monomer concentration, increasing VBPT concentration, lessening AIBN-to-VBPT ratio, or stopping polymerization at early stage. To confirm these assumptions, RAFT copolymerization using fixed VBPT and AIBN concentrations ($[VBPT]_0$:$[AIBN]_0$ = 10, $[AIBN]_0$ = 3.0 mmol/L) was conducted, and the results are shown in runs 16−19 of Table 1. As expected, RAFT copolymerization using low feed ratios (x = 5 and 10) afforded branched copolymers with polydispersity lower than 1.22, while the copolymerization at higher feed ratio gave branched copolymers with PDI beyond 1.36. These results could be ascribed to different rate of copolymerization originating from various MA concentrations. At a low feed ratio, the rate for addition−fragmentation chain transfer was slowed down due to low MA concentration; a large amount of unreacted trithiocarbonate functionality (P_1 > 45.6%) still remained in the resultant branched copolymer, and more molar fractions of VBPT could participate in the copolymerization, evident from significantly decreased monomer conversions and increased C_{M1}/C_{M2} values with lowered feed ratios. As x was increased from 5 to 50, both molecular weight and polydispersity were enhanced, and RB was gradually raised from 5.5 to 43. When the feed ratio was less than 20, the resultant branched copolymer had CTA functionality ranging between 8.52 and 11.0 and f_{CTA} beyond 0.9. Thus, branched copolymers with low polydispersity could be achieved as the copolymerization rate was slowed down.

Effects of Reaction Time on RAFT Copolymerization. Since the reactivity of the styryl group of VBPT varies with comonomers, it provides the versatility to synthesize branched copolymers via the RAFT process. The precise connectivity between individual branch and the distribution of branch length may be affected by factors such as feed ratio, monomer and initiator concentrations, temperature, and time. To investigate the effects of reaction time on polymerization, RAFT copolymerization using feed ratios of 0.4 and 100 and total monomer concentrations of 3.0 mol/L was conducted, and the results are listed in Tables 2 and 3, respectively.

For RAFT copolymerization using a feed ratio of 0.4 (Table 2), the VBPT conversion was gradually increased to 99.2% at 30 h, while MA was fully consumed in 12 h, suggesting different reactivity of VBPT and MA during copolymerization. The molecular weights of poly(VBPT-*co*-MA) branched copolymers obtained by GPC-MALLS tended to increase linearly

Table 2. Synthesis of Poly(VBPT-*co*-MA) Branched Copolymers by RAFT Copolymerization of VBPT (M_1) with MA (M_2) (x = 0.4)[a]

run	t (h)	C_{M1} (%)[b]	C_{M2} (%)[b]	M_n[c]	PDI[c]	RB(th)[d]	RB[e]	DB[e]	P_1 (%)[f]	P_2 (%)[f]	F[g]	f_{CTA}[h]
1	1	31.0	20.2	1280	1.22	1.26	5.74	0.174	78.2	10.5	5.37	0.998
2	2	58.4	44.9	1820	1.18	1.31	6.06	0.165	78.8	9.63	7.26	0.995
3	3	70.8	60.8	2560	1.24	1.34	6.19	0.162	79.0	9.27	10.6	0.991
4	6	79.6	90.7	3020	1.35	1.46	6.66	0.150	79.5	7.69	13.0	0.983
5	9	83.8	97.2	3350	1.48	1.46	6.65	0.150	80.4	4.35	15.6	0.970
6	12	87.0	100	3830	1.66	1.46	6.47	0.155	81.1	3.45	19.7	0.955
7	18	93.5	100	5260	2.01	1.43	6.30	0.159	82.2	3.32	32.6	0.941
8	24	97.6	100	6500	2.22	1.41	6.38	0.157	83.6	3.27	44.3	0.932
9	30	99.2	100	7800	2.35	1.40	6.55	0.153	85.3	3.15	55.8	0.921

[a] Polymerization conditions: $[MA]_0$:$[VBPT]_0$:$[AIBN]_0$ = 0.4:1:0.1, $[MA]_0 + [VBPT]_0$ = 3.0 mol/L, in toluene at 60 °C. [b] VBPT (C_{M1}) and MA (C_{M2}) conversions determined by ^{1}H NMR. The associated error in measuring integrated NMR signals for all polymer samples was estimated to be ±5%. [c] Determined by GPC-MALLS. [d] Theoretical repeat units per branch. [e] Determined by ^{1}H NMR. [f] Proportions of terminal trithiocarbonate functionality connecting with benzyl group (P_1) or MA unit (P_2) in branched copolymers. [g] Weight-average CTA functionality per branched copolymer. [h] Molar ratio of residual trithiocarbonate functionality in branched copolymer to VBPT participated in RAFT copolymerization.

Table 3. Synthesis of Poly(VBPT-*co*-MA) Branched Copolymers by RAFT Copolymerization of VBPT (M_1) with MA (M_2) (x = 100)[a]

run	t (h)	C_{M1} (%)[b]	C_{M2} (%)[b]	M_n(th,L)[c]	M_n[d]	PDI[d]	M_p(L)[e]	RB(th)[f]	RB[g]	F[h]	f_{CTA}[i]
1	2	54.8	12.1	2170	2 250	1.83	1 830	23.1	24.5	1.88	0.990
2	3.5	80.8	23.9	2810	4 120	1.55	2 670	30.6	33.1	2.23	0.984
3	5	90.2	36.7	3770	7 530	1.61	3 980	41.7	44.6	3.15	0.981
4	8	97.5	59.5	5520	12 600	1.50	6 360	62.0	64.7	3.30	0.963
5	12	100	83.3	7440	18 300	1.64	9 450	84.3	86.2	3.87	0.959
6	16	100	90.6	8070	20 400	1.80	10 200	91.6	93.5	4.22	0.928
7	24	100	95.9	8520	23 300	2.04	11 300	96.9	98.6	4.81	0.862
8	96	100	100	8880	30 700	2.43	12 200	101	101	6.29	0.749

[a] Polymerization conditions: $[MA]_0$:$[VBPT]_0$:$[AIBN]_0$ = 100:1:0.1, $[MA]_0 + [VBPT]_0$ = 3.0 mol/L, in toluene at 60 °C. [b] VBPT (C_{M1}) and MA (C_{M2}) conversions determined by ^{1}H NMR. The associated error in measuring integrated NMR signals for all polymer samples was estimated to be ±5%. [c] Theoretical molecular weight calculated by assuming VBPT was a normal RAFT agent and only linear chain was formed, $M_n(th,L) = MW_{VBPT} + MW_{MA} \times ([MA]_0/[VBPT]_0) \times C_{M2}/C_{M1}$. [d] Determined by GPC-MALLS. [e] Peak molecular weight of low molecular weight fraction in GPC traces. [f] Theoretical repeat units per branch. [g] Determined by ^{1}H NMR. [h] Weight-average CTA functionality per branched copolymer. [i] Molar ratio of residual trithiocarbonate functionality in branched copolymer to VBPT participated in RAFT copolymerization.

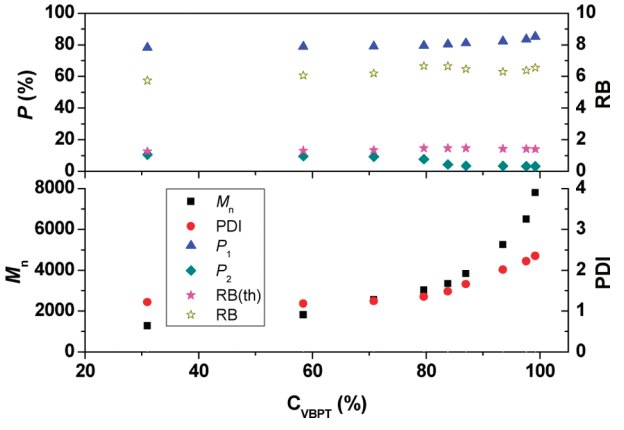

Figure 4. Dependence of M_n, PDI, P, and RB of poly(VBPT-*co*-MA) branched copolymers on VBPT conversion during RAFT copolymerization (x = 0.4). See Table 2 for detailed reaction conditions.

with VBPT conversion when VBPT conversion was below 87%, although gradually deviating from a linear evolution as VBPT conversion was further enhanced, due to increased radical−radical coupling reactions. In addition, polydispersity indices were observed to increase with enhanced conversion. The repeat units per branch only fluctuated between 5.7 and 6.7 (Figure 4), indicating the branches were oligomers with relatively narrow branch length distribution. The branched copolymers obtained at VBPT conversions below 70% had typical polydispersity around 1.2, thus indicating that branched copolymers with low polydispersity could be achieved by RAFT copolymerization at low MA-to-VBPT feed ratios and low conversions. With extended time, the molecular weight distributions of branched copolymers were observed to gradually broaden, as illustrated by the GPC traces in Figure 5. With increasing time, P_1 was slightly increased from 78.2% to 85.3%, and P_2 gradually decreased from 10.5% to 3.15%, reflecting the regular changes of end-group compositions with increased conversions. The F value up to reaction time was gradually increased from 5.37 to 55.8, and the loss of CTA functionality during copolymerization was not outstanding since the f_{CTA} values in Table 2 were usually higher than 0.92. These results confirmed that RAFT copolymerization performed at a low feed ratio could afford branched copolymers with near-adjustable branch length, branch length distribution, and a wide range of CTA functionalities.

dx.doi.org/10.1021/ma1024736 |*Macromolecules* 2011, 44, 2034–2049

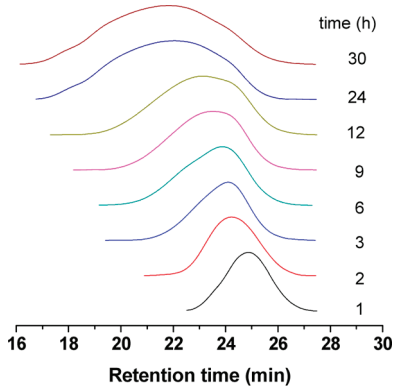

Figure 5. GPC traces of poly(VBPT-*co*-MA) branched copolymers obtained by RAFT copolymerization of VBPT with MA (x = 0.4) at various times. See Table 2 for detailed reaction conditions.

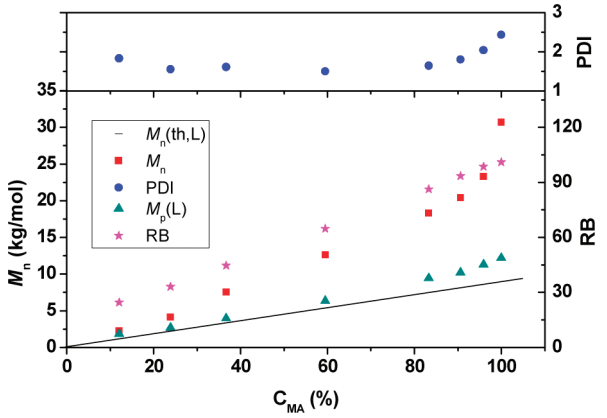

Figure 6. Dependence of M_n, PDI, and RB of poly(VBPT-*co*-MA) branched copolymers on VBPT conversion during RAFT copolymerization (x = 100). See Table 3 for detailed reaction conditions.

For RAFT copolymerization of VBPT with MA using a feed ratio of 100 (Table 3), both VBPT and MA conversions were increased with extended time; VBPT was fully consumed within 12 h, while it took more than 24 h to fully react MA. The RB values at various conversions were very close to the theoretical values, indicating the average repeat units per branch could be efficiently adjusted by control over monomer conversion. The significantly increased RB values with increasing time in Table 3 also revealed that the branch length was observed to increase with enhanced monomer conversion. The results were different from those obtained at a feed ratio of 0.4 in which the RB values were similar at various stages, which could be ascribed to different copolymerization behaviors originating from distinct reactivity of comonomers and feed ratios. When the feed ratio was 0.4, MA was more easily consumed, the branches were continuously formed until VBPT was completely polymerized, and the relatively low reactivity of VBPT unit in branched copolymer formed at high VBPT conversion further restricted side reactions, resulting in part loss of CTA functionality; thus, the RB values were similar. When the feed ratio was 100, VBPT was very limited in the copolymerization system and consumed faster than MA, which was used in large excess, and higher reactivity of MA resulted in the formation of a large amount of polymerizable linear chains with terminal styryl group (macro-CTA) at early

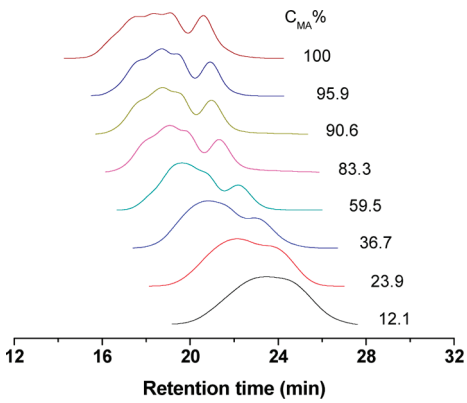

Figure 7. GPC traces of poly(VBPT-*co*-MA) branched copolymers obtained by RAFT copolymerization of VBPT with MA (x = 100) at various MA conversions.

stage. With increasing time, chain radicals further reacted with styryl group in macro-CTA or residual VBPT unit, leading to the formation of branched copolymer, while RB linearly increased with MA conversion due to large excess of MA monomer and relatively low branch numbers.

Figure 6 describes the dependence of M_n, PDI, RB of poly(VBPT-*co*-MA) branched copolymers, and peak molecular weight of low-molecular-weight fractions (M_p(L)) on MA conversion during RAFT copolymerization (x = 100), where M_n(th, L) is the theoretical molecular weight of linear chains calculated by assuming VBPT is a normal RAFT agent and has completely reacted at various conversions. The M_n values of the resultant branched copolymers tended to increase with extended time, and the polydispersity indices ranged between 1.50 and 2.43. Similar to typical RAFT polymerization, both M_p(L) and RB exhibited linear evolution with increasing MA conversion (C_{MA}). The molecular weight of branched copolymer was increased linearly with increasing MA conversion when C_{MA} was below 90.6% and then drastically increased at higher conversion. The RAFT copolymerization could be roughly divided into three stages. In the early stage (VBPT < 80.8%, MA% < 23.9%), VBPT was consumed rapidly due to its high chain transfer ability to MA, and at the beginning higher reactivity of MA resulted in the formation of polymerizable linear chains with terminal styryl group (macro-CTA). Meanwhile, star and branched copolymers were formed as styryl groups participated in the copolymerization. At this stage, there were a large amount of linear polymers in addition to star and branched copolymers, and GPC traces exhibited monomodal or double distributions (Figure 7). The weight-average CTA functionality per polymer was around 2, corresponding to very low DB value. In the second stage (VBPT% = 80.8−100%, MA% = 23.9−83.3%), the styryl group in residual VBPT and macro-CTA further participated in the RAFT process and formed the branching units; RAFT copolymerization was conducted until all the polymerizable styryl groups were completely consumed, and the branch numbers were gradually increased. The chain propagation originating from MA polymerization occurred smoothly, and multiple distributions appeared in GPC traces of the resultant polymers. In the last stage (VBPT % = 100%, MA% > 83.3%), residual MA further participated in the copolymerization, the branching units were mainly formed by side reactions such as termination and irreversible transfer, and the probability of coupling reaction between chain radicals

dx.doi.org/10.1021/ma1024736 |*Macromolecules* 2011, 44, 2034–2049

Table 4. Results for Copolymerization of VBPT (M_1) with Vinyl Monomers (M_2) via RAFT Process[a]

run	M_2	x	C_{M1} (%)[b]	C_{M2} (%)[b]	M_n[c]	PDI[c]	RB(th)[d]	RB[e]	DB[e]	P_1 (%)[f]	P_2 (%)[f]	F[g]	f_{CTA}[h]
1	St	1	81.3	60.5	16 300	2.65	1.74	3.71	0.270	56.8	34.3	117	0.932
2	St	100	99.5	58.3	9 990	1.60	59.6	59.6	0.0168	0	100	2.14	0.851
3	MMA	1	91.8	46.5	153 000	9.18	1.51	4.42	0.226	72.7	24.0	3997	0.907
4	MMA	100	100	52.6	138 500	1.88	53.6	89.1	0.0112	47.4	52.6	39.5	0.840
5	*t*BA	1	93.2	91.1	20 200	3.53	1.98	5.06	0.198	68.8	9.84	160	0.885
6	*t*BA	100	100	94.1	44 700	1.82	95.1	96.3	0.0104	1.55	92.6	5.16	0.782

[a] Polymerization conditions: $[M_2]_0$:$[VBPT]_0$:$[AIBN]_0 = x$:1:0.1, $[M_2]_0 + [VBPT]_0 = 3.0$ mol/L, in toluene at 80 °C for 30 h (runs 1 and 2) or at 60 °C for 24 h (runs 3−6). [b] VBPT (C_{M1}) and M_2 (C_{M2}) conversions determined by ^{1}H NMR. The associated error in measuring integrated NMR signals for all polymer samples was estimated to be ±5%. [c] Molecular weight and polydispersity determined by GPC-MALLS. [d] Theoretical repeat units per branch calculated by equation $RB(th) = ([M_2]_0 \times C_{M2})/([VBPT]_0 \times C_{M1}) + 1$. [e] Determined by ^{1}H NMR. [f] Proportions of terminal trithiocarbonate functionality connecting with benzyl group (P_1) or M_2 unit (P_2) in branched copolymers. [g] Weight-average CTA functionality per branched copolymer. [h] Molar ratio of residual trithiocarbonate functionality in branched copolymer to VBPT participated in RAFT copolymerization.

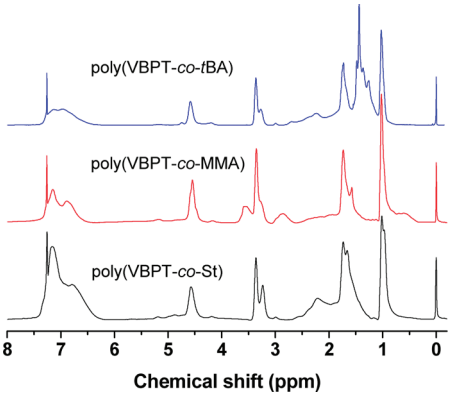

Figure 8. ^{1}H NMR spectra of various branched copolymers obtained by RAFT copolymerization ($[M_1]_0$:$[M_2]_0 = 1$).

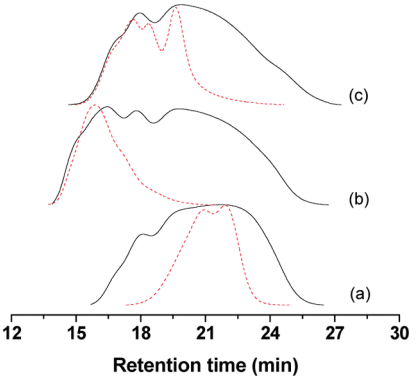

Figure 9. GPC traces of poly(VBPT-*co*-St) (a), poly(VBPT-*co*-MMA) (b), and poly(VBPT-*co*-*t*BA) (c) branched copolymers synthesized by RAFT copolymerization using various feed ratios: $[M_2]_0$:$[VBPT]_0 = 1$ (solid line) or 100 (dashed line).

was further increased due to lack of polymerizable monomer and increased viscosity of reaction mixtures, resulting in gradually decreased f_{CTA} values and significantly increased M_n and F values. The branched copolymers obtained at the last stage usually exhibited multiple distributions, high-molecular-weight fractions were noticeably increased, and the polydispersity indices were also correspondingly enhanced. Although molecular weight of branched copolymers could be further enhanced by using extended time to accelerate branch−branch coupling reactions, the ratio of M_w(LS) to M_p(L) in Table 3 only ranged between 1.9 and 8.4, suggesting the average branch numbers were not very high when a feed ratio of 100 was used. Branched copolymers with much higher M_n and DB values are possibly achieved in case of using multifunctional core reagents such as divinylbenzene and ethylene glycol dimethacrylate.

RAFT Copolymerization of VBPT with Other Vinyl Monomers. RAFT polymerization tolerates a wide range of monomers, so it is possible to generate a wide range of branched copolymers via copolymerization. To confirm the versatility and generality of this method, RAFT copolymerization of VBPT and other vinyl monomers such as methyl methacrylate (MMA), styrene (St), and *tert*-butyl acrylate (*t*BA) were also performed, and the results are listed in Table 4. The monomer conversions (*C*%) were determined by ^{1}H NMR by comparing the integrated areas of characteristic signals of monomer and polymer. In ^{1}H NMR spectra of poly(VBPT-*co*-M_2) (M_2 = MMA, St, and *t*BA) branched copolymers, the signals of CH_2S in VBPT unit with unreacted trithiocarbonate functionality and CHS in styryl unit originated from reacted VBPT appeared at about 4.56 and 4.18 ppm, the signals of CH_2S in terminal St and *t*BA unit appeared at 4.6−5.1 and 4.75 ppm, and the signals of CH_2 in terminal trithiocarbonate functionality were noted at around 3.36 ppm -(CH_2S, unreacted trithiocarbonate functionality), 3.27 ppm -(CH_2S, connected with terminal M_2 unit), and 2.99 ppm (CH_2S, connected with styryl unit originated from reacted VBPT) (Figure 8). On the basis of integrated analysis, proportions of terminal trithiocarbonate functionality connecting with benzyl group (P_1), M_2 unit (P_2), and styryl unit originated from reacted VBPT (P_3) in hyperbranched copolymers could be quantitatively determined.

For RAFT copolymerization using a comonomer of St or *t*BA, the DB and *F* values of branched copolymers obtained could be efficiently adjusted by control over comonomer feed ratios. RAFT copolymerization of VBPT with St using a feed ratio of 100 at 80 °C for 30 h gave a copolymer with polydispersity of 1.60, GPC traces exhibited double distribution (Figure 9), and CTA functionality was only 2.14, indicating the resultant copolymer was in fact mixtures of linear chains as well as star and branched polymers. This phenomenon could be ascribed to relatively low rate for reversible addition−fragmentation chain transfer polymerization of St; thus, extended time was necessary to further enhance the branch numbers. Other samples had variable polydispersity indices (1.88 < PDI < 9.18) and RB values (3.71 < RB < 96.3) and exhibited multiple distributions in GPC

dx.doi.org/10.1021/ma1024736 |*Macromolecules* 2011, 44, 2034–2049

Table 5. Solution Properties of Branched Polymers (Runs 1−13) and Linear Polymers (Runs 14−17)

run	polymer	$[VBPT]_0:[M_2]_0$[a]	M_n[b]	PDI[b]	$[\eta]_w$ (dL/g)[c]	α[d]	g'[e]	DB[f]
1	poly(VBPT-*co*-MA)	1	12 500	2.58	0.0672	0.366	0.250	0.154
2	poly(VBPT-*co*-MA)	5	17 600	2.60	0.109	0.386	0.324	0.117
3	poly(VBPT-*co*-MA)	10	18 700	2.02	0.149	0.487	0.502	0.0758
4	poly(VBPT-*co*-MA)	20	16 200	2.18	0.148	0.512	0.519	0.0448
5	poly(VBPT-*co*-MA)	50	19 000	2.02	0.179	0.539	0.597	0.0195
6	poly(VBPT-*co*-MA)	100	30 700	2.43	0.316	0.542	0.690	0.0099
7	poly(VBPT-*co*-St)	1	16 300	2.65	0.128	0.398	0.368	0.270
8	poly(VBPT-*co*-St)	100	9 990	1.60	0.123	0.623	0.741	0.0168
9	poly(VBPT-*co*-MMA)	1	153 000	9.18	0.433	0.422	0.189	0.226
10	poly(VBPT-*co*-MMA)	100	138 500	1.88	0.583	0.605	0.833	0.0112
11	poly(VBPT-*co*-*t*BA)	1	20 200	3.53	0.142	0.398	0.401	0.198
12	poly(VBPT-*co*-*t*BA)	100	44 700	1.82	0.279	0.511	0.721	0.0104
13	hyperbranched PVBPT[g]		24 700	5.94	0.158	0.360		
14	linear PMA[h]		70 800	2.11	0.708	0.632		
15	linear PSt[h]		24 300	1.55	0.316	0.740		
16	linear PMMA[h]		43 900	1.73	0.300	0.686		
17	linear P*t*BA[h]		99 000	1.94	0.683	0.659		

[a] Samples synthesized by RAFT copolymerization of VBPT with M_2 (M_2 = MA (runs 1−6), St (runs 7 and 8), MMA (runs 9 and 10) and *t*BA (runs 11 and 12)). [b] Determined by GPC-MALLS. [c] Weight-average intrinsic viscosity. [d] MHS exponent. [e] Contractor factor determined by equation $g' = [\eta]_b/[\eta]_l$. [f] Obtained by NMR analysis. [g] Obtained by RAFT SCVP conducted in toluene at 60 °C for 24 h ($[VBPT]_0$ = 3.0 mol/L, $[VBPT]_0:[AIBN]_0$ = 100). [h] Obtained by conventional free radical polymerization in toluene at 60 °C for 6 h ($[M]_0$ = 3.0 mol/L, $[M]_0:[AIBN]_0$ = 100).

traces, corresponding to the target branched copolymers. For poly(VBPT-*co*-MMA) branched copolymers, the RB values were significantly higher than the theoretical values, and the *F* value could reach up to 3997 ($x = 1$) due to different reactivity of MMA and VBPT and the presence of a large amount of unreacted trithiocarbonate groups in VBPT unit (P_1 = 47.4% or 72.7%) originating from relatively low chain transfer constant of VBPT to MMA. The chain transfer constants of trithiocarbonate-type CTA to methacrylates were typically lower than those to styrene, acrylates, and acrylamides, leading to poor control over RAFT polymerization of MMA.[78] For poly(VBPT-*co*-St) and poly(VBPT-*co*-*t*BA) branched copolymers synthesized by runs 1 and 5 using a low feed ratio (x = 1), repeat units per branch were also higher than the theoretical values, resulting from the presence of a large amount of unreacted trithiocarbonate groups in VBPT unit (P_1 > 56.8%) due to lack of polymerizable vinyl monomers. The f_{CTA} values of branched copolymers ranged between 0.782 and 0.932 (Table 4), revealing partial loss of CTA functionality during copolymerization. As a result, the target branched copolymers with variable DB and *F* values could be obtained by changing feed ratios and reaction time.

Solution Behavior of Branched Copolymers Obtained by RAFT Copolymerization. Some parameters such as Mark−Houwink−Sakurada (MHS) exponent (α) and contracting factor (g') are used to describe solution properties of branched polymers, which is distinctly different from their linear analogues due to their compact structures. The MHS exponent of branched polymer is smaller than that of the linear analogue, and the branching effect can be expressed by the contracting factor defined as $[\eta]_b/[\eta]_l$, where $[\eta]_b$ and $[\eta]_l$ are weight-average intrinsic viscosities of branched and linear polymers with same molecular weight, respectively.

In this study, the dependence of intrinsic viscosity on molecular weight was determined by GPC systems equipped with RI, viscosimetric, and multiangle light scattering detectors in THF at 35 °C. To aid with comparisons, linear polymers were synthesized by conventional free radical polymerization, and hyperbranched PVBPT was also obtained by RAFT SCVP. The solution properties of various linear and branched polymers are listed in Table 5. Typical Mark−Houwink−Sakurada plots of poly(VBPT-*co*-MA) branched copolymers, hyperbranched PVBPT, and linear PMA over a selected common molecular weight range are listed in Figure 10. Both the intrinsic viscosities and the MHS exponents of the branched copolymers were less than those of their linear reference. The MHS equation of various linear polymers was determined to be $[\eta]_l = 3.81 \times 10^{-4} M_w^{0.632}$ (linear PMA), $1.29 \times 10^{-4} M_w^{0.740}$ (linear PSt), $1.35 \times 10^{-4} M_w^{0.686}$ (linear PMMA), and $2.25 \times 10^{-4} M_w^{0.659}$ (linear P*t*BA), and the MHS equation of hyperbranched PVBPT was obtained to be $[\eta]_b = 2.18 \times 10^{-3} M_w^{0.360}$. For poly(VBPT-*co*-MA)

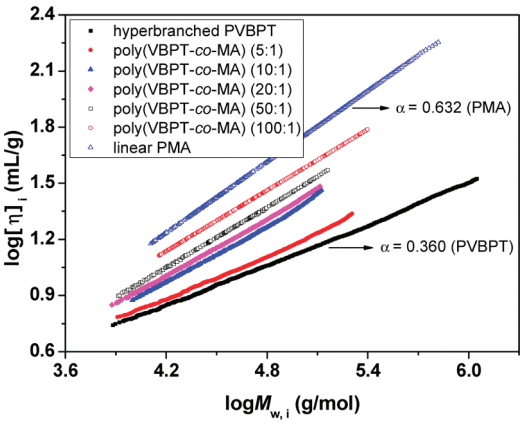

Figure 10. Mark−Houwink−Sakurada plots of poly(VBPT-*co*-MA) branched copolymers obtained by RAFT copolymerization using different MA-to-VBPT feed ratios, hyperbranched PVBPT, and linear PMA. The resulting α values were determined from the slope.

dx.doi.org/10.1021/ma1024736 |*Macromolecules* 2011, 44, 2034–2049

Table 6. Synthesis of Star-Shaped Polymers by RAFT Polymerization Mediated by Poly(VBPT-*co*-MA) Branched Copolymers[a]

run	M	DP_0	$[AIBN]_0$ (mmol/L)	t (h)	C%	M_n(th)[b]	M_n[c]	PDI[c]	M_n(NMR)[d]	$[\eta]_s$ (dL/g)[e]	g'[f]
1	St	100	0.50	10	5.45	10 400	10 800	1.21	10 600	0.0532	0.369
2	St	100	1.0	10	9.64	16 100	17 500	1.32	16 200	0.0768	0.351
3	St	100	2.0	10	13.1	20 800	21 100	1.35	20 500	0.085	0.333
4	St	100	4.0	10	20.2	30 400	36 200	1.88[g]	30 500	0.159	0.327
5	St	200	1.0	10	7.87	24 300	27 500	1.42[g]	25 600	0.104	0.323
6	St	400	1.0	10	10.4	59 300	67 200	1.65[g]	61 300	0.218	0.312
7	*t*BA	100	2.0	8	42.8	74 300	78 300	1.25	75 700	0.138	0.315
8	St	200	1.0	18	25.6	40 500	42 200	1.18	42 100	0.198	0.513
9	*t*BA	200	1.0	18	53.5	101 400	112 000	1.12	108 000	0.256	0.497
10	St	100	1.0	18	20.2	125 200	149 000	1.72[g]	123 000	0.172	0.132
11	*t*BA	50	1.6	24	73.2	269 600	298 000	1.55[g]	271 000	0.143	0.117

[a] Reaction conditions: $DP_0 = [M]_0/(F[\text{macro-CTA}]_0)$, $[M]_0$ = 2.0 mol/L (runs 1−10) or 0.80 mol/L (run 11), in toluene (for St) or acetone (for *t*BA) at 60 °C, and macro-CTAs were poly(VBPT-*co*-MA) branched copolymers with various molecular weight and polydispersity: runs 1−7, M_n = 3020, PDI = 1.35, F = 13.0; runs 8 and 9, M_n = 1820, PDI = 1.18, F = 7.26; runs 10 and 11, M_n = 7800, PDI = 2.35, F = 55.8. [b] Theoretical molecular weight, M_n(th) = M_n(macro-CTA) + $MW_M \times ([M]_0/[\text{macro-CTA}]_0) \times$ conversion. [c] Molecular weight and polydispersity of star polymers determined by GPC-MALLS. [d] Molecular weight estimated by ^{1}H NMR by assuming no CTA functionality was lost during polymerization, M_n(NMR) = M_n(CTA) + $104.15 \times F \times 2(I_{6.2-7.5} - 2I_{3.25})/5I_{3.25}$ (for star PSt) or M_n(CTA) + $128.17 \times F \times 2I_{2.22}/I_{3.32}$ (for star P*t*BA). [e] Weight-average intrinsic viscosity. [f] Contractor factor determined by equation $g' = [\eta]_s/[\eta]_l$, $[\eta]_l = 1.29 \times 10^{-4} M_w^{0.740}$ (linear PSt) and $2.25 \times 10^{-4} M_w^{0.659}$ (linear P*t*BA). [g] Shoulders or multiple distributions appeared in GPC traces.

branched copolymers synthesized by RAFT copolymerization, when the MA-to-VBPT feed ratio increased from 1 to 100, the α values increased from 0.366 to 0.542, and the g' values increased from 0.25 to 0.69. A similar tendency was observed for other branched copolymers obtained by RAFT copolymerization using feed ratios of 1 and 100 (see the Supporting Information). These observations are consistent with the DB results obtained by NMR spectra, which further indicated that the branching nature of the resultant copolymers was directly related to the amount of branching agent participated in the copolymerization. The above results are in good agreement with the solution properties of branched poly(*N*-isopropylacrylamide) reported by Vogt and Sumerlin.[58]

Synthesis of Star-Shaped Polymers by RAFT Polymerization Mediated by Multifunctional Branched Chain Transfer Agents. Branched copolymers synthesized by RAFT copolymerization using low feed ratios possessed a wide range of CTA functionalities, thus they could be used as multifunctional RAFT agents to prepare star-shaped polymers and polymer networks[26−29] with a branched core. In this study, star PSt and P*t*BA were synthesized by RAFT polymerization mediated by poly(VBPT-*co*-MA) branched copolymers obtained by RAFT copolymerization of VBPT with MA using a feed ratio of 0.4, and their F values were 7.26 (runs 8 and 9), 13.0 (runs 1−7), and 55.8 (runs 10 and 11), respectively (Table 6). In Table 6, molecular weight of star polymers determined by ^{1}H NMR (M_n(NMR)) was calculated by assuming that the average CTA functionality per polymer did not change during RAFT polymerization. As the reaction time was beyond 5 h, the signals of CHS of terminal MA unit at 4.87 ppm, CH_2S of VBPT unit at 4.56 ppm, and CHS of styryl unit at 4.18 ppm corresponding to groups connecting with trithiocarbonate moieties wholly disappeared, and new signals of CHS (terminal St unit at 5.12 ppm and terminal *t*BA unit at 4.68 ppm) were quantitatively noted in ^{1}H NMR spectra of star polymers obtained, indicating these remaining CTA functionalities had completely participated in RAFT process to perform chain propagation. The signals of CH_2S corresponding to terminal CTA functionality of star PSt and P*t*BA appeared at

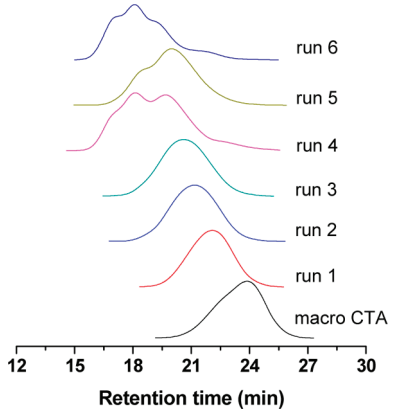

Figure 11. GPC traces of poly(VBPT-*co*-MA) branched copolymer and PSt stars with a branched core synthesized by runs 1−6 in Table 6.

3.25 and 3.32 ppm, and their characteristic signals were noted at 6.2−7.5 (Ar*H*, PSt), 2.22 (C*H*, P*t*BA), and 1.44 ppm (CH_3O, P*t*BA); thus, the degree of polymerization per arm was obtained. The average arm number of the resultant star polymers could be determined by the CTA functionality of branched cores if no end-functionality was lost during polymerization.

First, poly(VBPT-*co*-MA) branched copolymer (M_n = 3020, PDI = 1.35, F = 13.0) was used as multifunctional CTA to mediate RAFT polymerization of St and *t*BA, and effects of feed ratio and initiator concentration on polymerization were investigated. By comparing results listed in runs 1−4 in Table 6, it can be seen monomer conversion increased with AIBN concentration, and M_n(NMR) of star PSt obtained was very close to the expected value. When AIBN concentration was increased from 0.5 to 2 mmol/L, the polydispersity indices was slightly enhanced from 1.21 to 1.35, and GPC traces exhibited monomodal distribution; when it was increased to 4 mmol/L, the PDI of star PSt reached up to 1.88, and multiple distributions appeared in GPC trace (Figure 11), corresponding to obvious star−star coupling. As $[M]_0/(F[\text{CTA}]_0)$ increased from 100 to 400, RAFT

polymerization at 10 h gave similar monomer conversions, the PDI values of the resultant stars were increased from 1.32 to 1.65, and a shoulder or multiple distributions appeared in GPC traces of star PSt obtained at high feed ratios. These results indicated star−star coupling became more pronounced with increasing feed ratio and initiator concentration, and the critical degree of polymerization per arm to start intermolecular coupling (DP*) was estimated to be about 16.7 (run 5). RAFT polymerization of *t*BA at 8 h afforded star P*t*BA with adjustable molecular weight and low polydispersity (PDI = 1.25), suggesting the DP* value for *t*BA polymerization was much higher than that for St polymerization.

Then poly(VBPT-*co*-MA) branched copolymers with CTA functionalities of 7.26 and 55.8 were used to mediate RAFT polymerization, and the results are shown in runs 8−11 of Table 6. In runs 8 and 9, the molecular weights of star polymers were close to the theoretical values, and the PDI values were lower than 1.2. No significant shoulders and tailings were noted in GPC traces, corresponding to neglectable side reactions during polymerization. The DP* value for St polymerization was estimated to be higher than 53.3 when F was 7.26. In runs 10 and 11 using branched copolymer with CTA functionality up to 55.8, the PDI values were higher than 1.55, and multiple distributions appeared in GPC traces of star polymers, corresponding to serious intermolecular coupling. In this case, the M_n(NMR) values of star polymers was lower than the real values since average arm numbers of star polymers obtained were higher than the original CTA functionality. The DP* values for St polymerization were observed to decrease with increasing CTA functionality of multifunctional RAFT agents, which could be ascribed to relatively high radical concentrations and increased activity of polymer radicals originating from enhanced arm numbers.

It is necessary to further investigate the evolution of grafting efficiency during star polymer formation. To cleave the arms from star polymers is the way of choice to determine the average arm number of star polymer and the uniformity of each arm.[72−77] However, the branched core herein was R group of the macro-RAFT agents; therefore, the attached PSt or P*t*BA chains (arms) could not be cleaved from the resultant star polymers via hydrolysis or aminolysis. In this study, an indirect way was introduced to elucidate star architectures of the resulting polymers. The intrinsic viscosities ($[\eta]_s$) were measured in THF at 35 °C and compared with those of linear PSt or P*t*BA with same molecular weights calculated by the following equations: $[\eta]_l = 1.29 \times 10^{-4} M_w^{0.740}$ (linear PSt) and $2.25 \times 10^{-4} M_w^{0.659}$ (linear P*t*BA). The branching parameter g' defined as $[\eta]_s/[\eta]_l$ of each sample is listed in Table 6. The g' values were compared with those calculated by equations proposed by Roovers[79] (eq 1) and Douglas et al.[80] (eq 2), where f stands for arm number of star polymers.

$$\log g' = 0.36 - 0.8 \log f \quad (1)$$

$$g' = \{[(3f-2)/f^2]^{0.58}[0.724 - 0.015(f-1)]\}/0.724 \quad (2)$$

For regular star-shaped polymers, the g' values deduced from eq 1 were 0.469 (f = 7.26), 0.294 (f = 13.0), and 0.0918 (f = 55.8), and the g' values calculated from eq 2 were 0.493 (f = 7.26) and 0.311 (f = 13.0). From Table 6, it can be seen the g' values experimentally determined were slightly higher than those calculated. There are two possible reasons to account for the deviation. One reason is the overestimated arm number of star polymers since the F value was defined as weight-average CTA functionality per polymer in this study; another reason is the nonexact arm number of star polymers due to complex structures of macro-CTAs formed by RAFT SCVP. The experimental g' values of star polymers were close to those calculated from the well-proven theoretical model, suggesting the arm numbers of various star polymers were similar to the CTA functionalities of branched macro-CTAs.

The above results demonstrated that star polymers with adjustable molecular weight, relatively low polydispersity and variable arm numbers could be achieved by two successive RAFT processes, in which star−star coupling reactions could be further restricted by optimum conditions to slow down polymerization rate.[53] RAFT copolymerization of VBPT with vinyl monomers could afford branched copolymers with CTA functionality varying from 3 to 107 or more (Table 1); thus, the subsequent RAFT polymerization possibly enables the synthesis of star polymers with a wide range of arm numbers and arm lengths, and star block copolymers are expected to be obtained by chain extension polymerization. As compared with traditional core first method in which the multifunctional core is usually synthesized by multiple organic reactions, the branched core obtained in this study can be achieved by one-step RAFT process, and the CTA functionality can be adjusted by control over feed ratio of VBPT to normal vinyl monomers, monomer and initiator concentrations as well as reaction time; thus, this alternative method may be more promising for the synthesis of star polymers due to its generality and versatility. The arm number of the resultant star polymers dependent on branched RAFT agents obtained by RAFT copolymerization via SCVP was not very exact, and the uncertain arm number of star polymers is similar to that obtained using the arm first method. It should be mentioned the real structures of star polymers obtained by the arm first method are more complex although the arm length is uniform since the formed core usually has uncontrollable molecular weight and high polydispersity.[59−63] In this study, however, the branched core obtained under optimized conditions has adjustable molecular weight, low polydispersity, and variable CTA functionality, and the versatility of RAFT copolymerization enables the introduction of other functional groups such as hydroxyl, carbonyl, alkyl halide, epoxy, succinic anhydride, amine, and fluorescent moiety into branched copolymer;[81−85] thus, a variety of macromolecular architectures are possibly achieved by subsequent "living"/controlled polymerization and postmodification reaction. This alternative approach could be exploited to synthesize stimuli-responsive star and branched polymers; synthesis and properties of other functional polymers are currently under way in our laboratory.

Thermal Properties of Typical Branched Copolymers. The thermal properties of star and branched polymers were usually different from their linear analogues due to the branching effect. In this study, the thermal properties of typical branched copolymers were characterized by DSC and TGA, and the results are listed in Table 7. Glass transition temperature (T_g) of branched copolymers may be affected by some factors such as branch number, repeat units per branch, chemical composition, and polydispersity. In DSC curves of poly(VBPT-*co*-MA) branched copolymers (Figure 12), only one T_g ranging between 13.0 and 25.3 °C was noted, suggesting good compatibility of VBPT and MA units in branched copolymers. Theoretically, increased chain length always results in enhanced T_g due to more restricted chain mobility, and the branching effect also significantly affects T_g

Table 7. Thermal Properties of Typical Poly(VBPT-*co*-M_2) Branched Copolymers

entry	M_2	x	t (h)	M_n	PDI	RB	F	T_g (°C)[a]	T_{max} (°C)[b]
1	MA	0.5	96	11 800	3.09	6.32	107	25.3	290.5, 420.2
2	MA	5	96	17 600	2.60	8.55	59.3	16.3	286.4, 419.4
3	MA	10	96	18 700	2.02	13.2	28.8	13.0	285.2, 416.6
4	MA	20	96	16 200	2.18	22.3	14.7	14.9	288.4, 413.0
5	MA	50	96	19 000	2.02	51.3	6.36	13.7	285.5, 408.6
6	MA	100	96	30 700	2.43	101	6.29	16.4	302.1, 407.2
7	St	1	24	16 300	2.65	3.71	117	53.3	294.3, 403.5
8	St	100	24	9 990	1.60	59.6	2.14	92.3	294.4, 415.4
9	MMA	1	24	153 000	9.18	4.42	3997	55.7	294.5, 412.5
10	MMA	100	24	138 500	1.88	89.1	39.5	128.4	307.1, 398.2
11	*t*BA	1	24	20 200	3.53	5.06	160	31.3	244.2, 289.7, 416.4
12	*t*BA	100	24	44 700	1.82	96.3	5.16	46.9	241.6, 270.2, 438.7

[a] Determined by DSC. [b] Determined by differential analysis derived from TGA curves.

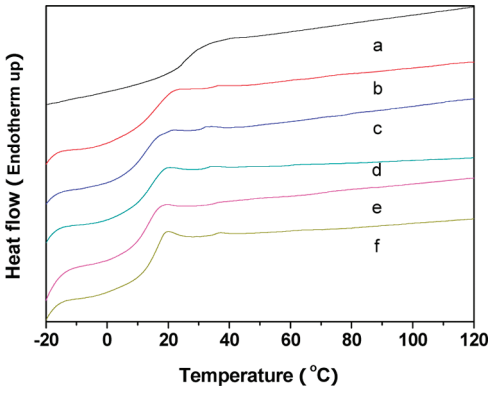

Figure 12. DSC traces of poly(VBPT-*co*-MA) branched copolymers synthesized by using different feed ratios: x = 0.5 (a), 5 (b), 10 (c), 20 (d), 50 (e), and 100 (f).

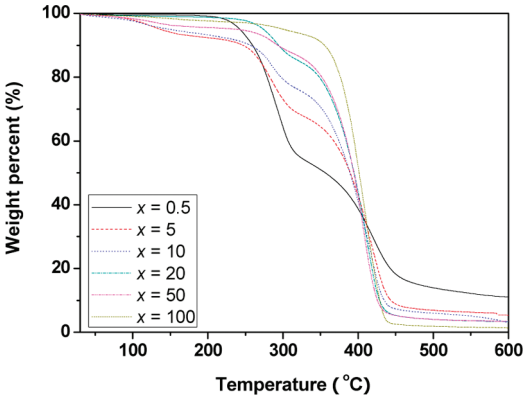

Figure 13. TGA curves of poly(VBPT-*co*-MA) branched copolymers synthesized by RAFT copolymerization at various feed ratios.

values. Polymers with more branches have enhanced free volumes due to increased chain ends, which will reduce T_g. Meanwhile, the branches also hinder the chain mobility, like bulky side groups, which will increase T_g. The T_g values in entries 2−6 of Table 7 were similar, suggesting all these factors almost counteract with each other. A significant increased T_g of 25.3 °C was noted in entry 1, and DSC curve exhibited a wide temperature range for glass transition, which could be ascribed to the significantly restricted chain mobility due to the presence of a large number of branches. In TGA curves of poly(VBPT-*co*-MA) branched copolymers (Figure 13), two obvious decomposition stages were observed. The first stage in which the maximum decomposition temperatures (T_{max}) appeared between 285 and 302 °C could be ascribed to decomposition of trithiocarbonate functionality in terminal groups or side chains of branched copolymers. At second stage ranging from 320 to about 450 °C, the residual polymers containing MA units and aromatic derivatives originating from VBPT units were subjected to further decomposition. T_{max} corresponding to second-stage decomposition was observed to decrease with increasing feed ratios; namely, poly(VBPT-*co*-MA) branched copolymers with more VBPT units possessed enhanced thermal stability even if they had shorter branch length, indicating the strong dependence of thermal stability on chemical composition of branched copolymers.

For other branched copolymers comprising St, MMA, and *t*BA units, one obvious T_g was noted in the DSC curves (Figure 14), indicating all these branched copolymers were miscible. The chain relaxation of branched copolymers was more complex than that of their linear analogues, and some secondary transition signals were sometimes noticeable in DSC traces. For instance, in addition to a major transition corresponding to T_g, two secondary relaxation signals were noted at 22.9 and 36.8 °C (for branched poly(VBPT-*co*-St) obtained at x = 1), 17.9 and 33.0 °C (for branched poly(VBPT-*co*-St) obtained at x = 100), and 35.4 and 76.2 °C (for branched poly(VBPT-*co*-MMA) obtained at x = 100). Careful inspection of T_g values in runs 7−12 in Table 6 noted branched copolymers obtained at feed ratio of 100 had T_g values significantly higher than those obtained at feed ratio of 1, which may originate from their different branch length, branch number, and chemical components. In the TGA curves of these branched copolymers (Figure 15), two or three stages of thermal decomposition were observed. The thermal stability of various branched copolymers was also different, suggesting its strong dependence on topology and chemical components. In the TGA curves of poly(VBPT-*co*-St) and poly(VBPT-*co*-MMA) branch copolymers, the first stage with a T_{max} of around 294 °C could be primarily attributed to decomposition of trithiocarbonate functionality in branched copolymers, and the second stage beyond 320 °C mainly corresponded to the

dx.doi.org/10.1021/ma1024736 |*Macromolecules* 2011, 44, 2034–2049

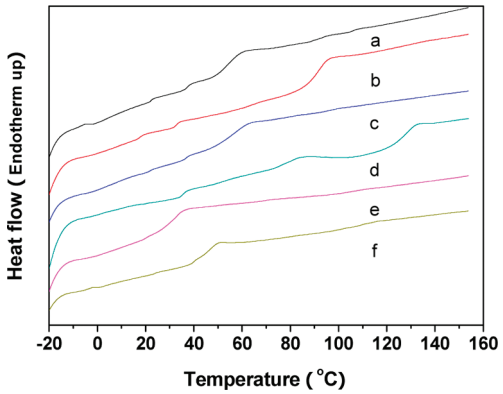

Figure 14. DSC traces of poly(VBPT-*co*-St) (a, b), poly(VBPT-*co*-MMA) (c, d), and poly(VBPT-*co*-*t*BA) (e, f) branched copolymers obtained by RAFT copolymerization using feed ratios of 1 (a, c, and e) or 100 (b, d, and f).

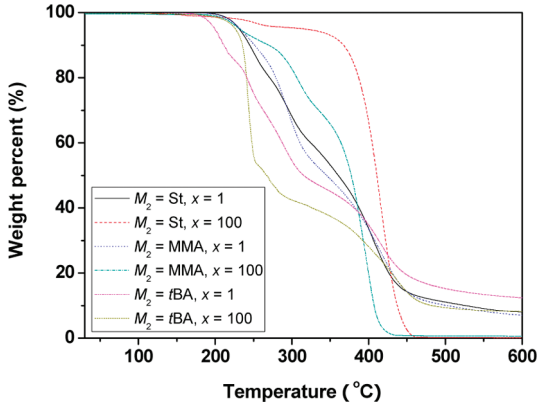

Figure 15. TGA curves of poly(VBPT-*co*-St), poly(VBPT-*co*-MMA), and poly(VBPT-*co*-*t*BA) branched copolymers synthesized by RAFT copolymerization using feed ratios of 1 and 100.

decomposition of the residual polymers with St or MMA units and aromatic derivatives originating from VBPT units. Three decomposition stages for poly(VBPT-*co*-*t*BA) branched copolymers were noted in the TGA curves. The first stage appeared between 180 and 250 °C, and the second stage was noted between 250 and 320 °C, both stages primarily originated from side-group decomposition of *t*BA units and decomposition of trithiocarbonate functionality. The residual chains were then further decomposed at the last stage beyond 320 °C.

The above results indicated that RAFT copolymerization seemed to improve the compatibility of polymer segments with relatively different polarity and afforded branched copolymers without noticeable phase separation under certain conditions.

CONCLUSION

Synthesis of branched and star polymers on the basis of VBPT via 1−2 step RAFT process(es) was investigated. Branched copolymers with controlled chemical components, degree of branching, and variable CTA functionality were synthesized by RAFT copolymerization of VBPT with vinyl monomers. Effects of comonomer feed ratio, monomer and initiator concentrations, and reaction time on RAFT copolymerization of VBPT with MA were investigated, and it was found that repeat units per branch and chemical compositions of terminal groups of branched copolymers obtained could be adjusted by control over feed ratio and reaction time. Molecular weights of branched copolymers were liable to increase with increasing vinyl monomer-to-VBPT feed ratio and reaction time; however, copolymerization behaviors at high and low feed ratios were noticeably different. RAFT copolymerization of VBPT with MA at a low feed ratio of 0.4 afforded hyperbranched copolymers with RB values only fluctuated between 5.7 and 6.7 due to the presence of a large amount of VBPT units with unreacted trithiocarbonate moieties, while RAFT copolymerization using a high feed ratio of 100 gave branched copolymers with RB values similar to the expected values. RAFT copolymerization was a versatile method to synthesize branched copolymers with variable branch numbers and CTA functionalities and a wide range of molecular weight distributions (1.16 < PDI < 9.18), which were macro-RAFT agents of choice to synthesize star-shaped polymers. Poly(VBPT-*co*-MA) branched copolymers with CTA functionalities of 7.26, 13.0, and 55.8 were used to mediate RAFT polymerization of St and *t*BA, and star polymers with controllable molecular weight and variable polydispersity (1.12 < PDI < 1.88) were obtained. The approach based on two successive RAFT processes is general and versatile to synthesize star-shaped polymers with variable chemical components and arm numbers similar to the original branched macro-CTAs although the arm number is not very exact. The resultant hyperbranched and star-shaped polymers were characterized by ^{1}H NMR, GPC-MALLS, DSC, and TGA. Both α and g' values of branched copolymers were observed to increase with increasing feed ratio of vinyl monomer to VBPT, indicating that the branching nature of the resultant copolymers was directly related to the amount of branching agent participated in the copolymerization. Thermal properties of branched copolymers were dependent on factors such as chemical components, branch number, branch length, and molecular weight distribution, and the single glass transition temperature observed in DSC analyses confirmed that branched copolymers obtained at various feed ratios had good compatibility.

ASSOCIATED CONTENT

Supporting Information. NMR spectra of VBPT, PMA, and star polymers, IR spectra of VBPT and star polymers, TGA curve of VBPT, GPC traces of branched copolymers and star P*t*BA, and Mark−Houwink−Sakurada plots of other branched copolymers and their linear analogues. This material is available free of charge via the Internet at http://pubs.acs.org.

AUTHOR INFORMATION

Corresponding Author
*Fax +86 512 65882045; e-mail ylzhao@suda.edu.cn.

ACKNOWLEDGMENT

The financial support from the National Natural Science Foundation of China (Grants 20844001, 20874067, and 21074081), the Key Project of Chinese Ministry of Education (No. 209049), Natural Science Fund for Colleges and Universities of Jiangsu Province (No. 08KJB150015), and the Undergraduate Research and Innovation Plan of Jiangsu Province (No. 57315891) is gratefully acknowledged. The authors are grateful

to the kind help from Prof. Junpo He and Dr. Chao Zhang at Fudan University.

REFERENCES

(1) Hadjichristidis, N.; Pitsikalis, M.; Pispas, S.; Iatrou, H. *Chem. Rev.* **2001**, *101*, 3747.
(2) Hirao, A.; Hayashi, M.; Loykulnant, S.; Sugiyama, K.; Ryu, S. W.; Haraguchi, N.; Matsuo, A.; Higashihara, T. *Prog. Polym. Sci.* **2005**, *30*, 111.
(3) Gao, C.; Yan, D. Y. *Prog. Polym. Sci.* **2004**, *29*, 183.
(4) Voit, B. I.; Lederer, A. *Chem. Rev.* **2009**, *109*, 5924.
(5) Li, Z. B.; Kesselman, E.; Talmon, Y.; Hillmyer, M. A.; Lodge, T. P. *Science* **2004**, *306*, 98.
(6) Wang, G. W.; Hu, B.; Huang, J. L. *Macromolecules* **2010**, *43*, 6939.
(7) Zhang, Y. F.; Li, C. H.; Liu, S. Y. *J. Polym. Sci., Part A: Polym. Chem.* **2009**, *47*, 3066.
(8) Peng, Y.; Liu, H. W.; Zhang, X. Y.; Liu, S. Y.; Li, Y. S. *Macromolecules* **2009**, *42*, 6457.
(9) Zhao, Y. L.; Cai, Q.; Jiang, J.; Shuai, X. T.; Bei, J. Z.; Chen, C. F.; Xi, F. *Polymer* **2002**, *43*, 5819.
(10) Zhao, Y. L.; Shuai, X. T.; Chen, C. F.; Xi, F. *Chem. Mater.* **2003**, *15*, 2836.
(11) Zhao, Y. L.; Chen, Y. M.; Chen, C. F.; Xi, F. *Polymer* **2005**, *46*, 5808.
(12) Zhao, Y. L.; Shuai, X. T.; Chen, C. F.; Xi, F. *Macromolecules* **2004**, *37*, 8854.
(13) Zhao, Y. L.; Shuai, X. T.; Chen, C. F.; Xi, F. *Chem. Commun.* **2004**, 1608.
(14) Zhao, Y. L.; Higashihara, T.; Sugiyama, K.; Hirao, A. *J. Am. Chem. Soc.* **2005**, *127*, 14158.
(15) Zhao, Y. L.; Higashihara, T.; Sugiyama, K.; Hirao, A. *Macromolecules* **2007**, *40*, 228.
(16) Wang, X.; He, J. P.; Yang, Y. L. *J. Polym. Sci., Part A: Polym. Chem.* **2007**, *45*, 4818.
(17) Gao, H. F.; Matyjaszewski, K. *Prog. Polym. Sci.* **2009**, *34*, 317.
(18) Rodionov, V.; Gao, H. F.; Scroggins, S.; Unruh, D. A.; Avestro, A. J.; Fréchet, J. M. J. *J. Am. Chem. Soc.* **2010**, *132*, 2570.
(19) Konkolewicz, D.; Gray-Weale, A.; Perrier, S. *J. Am. Chem. Soc.* **2009**, *131*, 18075.
(20) Kakwere, H.; Perrier, S. *J. Polym. Sci., Part A: Polym. Chem.* **2009**, *47*, 6396.
(21) Semsarilar, M.; Ladmiral, V.; Perrier, S. *Macromolecules* **2010**, *43*, 1438.
(22) Jiang, X. B.; Chen, Y. M.; Xi, F. *Macromolecules* **2010**, *43*, 7056.
(23) Stenzel, M. H. *Macromol. Rapid Commun.* **2009**, *30*, 1603.
(24) England, R. M.; Rimmer, S. *Polym. Chem.* **2010**, *1*, 1533.
(25) Shepherd, J.; Sarker, P.; Swindells, K.; Douglas, I.; MacNeil, S.; Swanson, L.; Rimmer, S. *J. Am. Chem. Soc.* **2010**, *132*, 1736.
(26) Kafouris, D.; Gradzielski, M.; Patrickios, C. S. *Macromol. Chem. Phys.* **2009**, *210*, 367.
(27) Kafouris, D.; Gradzielski, M.; Patrickios, C. S. *J. Polym. Sci., Part A: Polym. Chem.* **2008**, *46*, 3958..
(28) Themistou, E.; Patrickios, C. S. *Eur. Polym. J.* **2007**, *43*, 84.
(29) Vamvakaki, M.; Patrickios, C. S. *Chem. Mater.* **2006**, *14*, 1630.
(30) Wolf, K. W.; Frey, H. *Macromolecules* **2009**, *42*, 9443.
(31) Gottschalk, C.; Frey, H. *Macromolecules* **2006**, *39*, 1719.
(32) Hong, C. Y.; You, Y. Z.; Wu, D. C.; Liu, Y.; Pan, C. Y. *J. Am. Chem. Soc.* **2007**, *129*, 5354.
(33) Fréchet, J. M. J.; Henmi, M.; Gitsov, I.; Aoshima, S.; Leduc, M. R.; Grubbs, R. B. *Science* **1995**, *269*, 1080.
(34) Hawker, C. J.; Fréchet, J. M. J.; Grubbs, R. B.; Dao, J. *J. Am. Chem. Soc.* **1995**, *117*, 10763.
(35) Matyjaszewski, K.; Gaynor, S. G.; Kulfan, A.; Podwika, M. *Macromolecules* **1997**, *30*, 5192.
(36) Matyjaszewski, K.; Gaynor, S. G.; Müller, A. H. E. *Macromolecules* **1997**, *30*, 7034.
(37) Simon, P. F. W.; Müller, A. H. E.; Pakula, T. *Macromolecules* **2001**, *34*, 1677.
(38) Liu, B.; Kazlauciunas, A.; Guthrie, J. T.; Perrier, S. *Macromolecules* **2005**, *38*, 2131.
(39) Liu, B.; Kazlauciunas, A.; Guthrie, J. T.; Perrier, S. *Polymer* **2005**, *46*, 6293.
(40) Otsu, T. *J. Polym. Sci., Part A: Polym. Chem.* **2000**, *38*, 2121.
(41) Hawker, C. J.; Bosman, A. W.; Harth, E. *Chem. Rev.* **2001**, *101*, 3661.
(42) Matyjaszewski, K.; Xia, J. *Chem. Rev.* **2001**, *101*, 2921.
(43) Kamigaito, M.; Ando, T.; Sawamoto, M. *Chem. Rev.* **2001**, *101*, 3689.
(44) Ouchi, M.; Terashima, T.; Sawamoto, M. *Chem. Rev.* **2009**, *109*, 4963.
(45) Moad, G.; Rizzardo, E.; Thang, S. H. *Aust. J. Chem.* **2005**, *58*, 379.
(46) Perrier, S.; Takolpuckdee, P. *J. Polym. Sci., Part A: Polym. Chem.* **2005**, *43*, 5347.
(47) Boyer, C.; Bulmus, V.; Davis, T. P.; Ladmiral, V.; Liu, J. Q.; Perrier, S. *Chem. Rev.* **2009**, *109*, 5402.
(48) Barner-Kowollik, C.; Perrier, S. *J. Polym. Sci., Part A: Polym. Chem.* **2008**, *46*, 5715.
(49) Barner, L.; Davis, T. P.; Stenzel, M. H.; Barner-Kowollik, C. *Macromol. Rapid Commun.* **2007**, *28*, 539.
(50) Stenzel, M. H.; Davis, T. P. *J. Polym. Sci., Part A: Polym. Chem.* **2002**, *40*, 4498.
(51) Stenzel, M. H.; Davis, T. P.; Barner-Kowollik, C. *Chem. Commun.* **2004**, 1546.
(52) Hao, X. J.; Nilsson, C.; Jesberger, M.; Stenzel, M. H.; Malmström, E.; Davis, T. P.; Ostmark, E.; Barner-Kowollik, C. *J. Polym. Sci., Part A: Polym. Chem.* **2004**, *42*, 5877.
(53) Chaffey-Millar, H.; Stenzel, M. H.; Davis, T. P.; Coote, M. L.; Barner-Kowollik, C. *Macromolecules* **2006**, *39*, 6406.
(54) Bernard, J.; Favier, A.; Davis, T. P.; Barner-Kowollik, C.; Stenzel, M. *Polymer* **2006**, *47*, 1073.
(55) Wang, Z. M.; He, J. P.; Tao, Y. F.; Yang, L.; Jiang, H. J.; Yang, Y. L. *Macromolecules* **2003**, *36*, 7446.
(56) Carter, S.; Hunt, B.; Rimmer, S. *Macromolecules* **2005**, *38*, 4595.
(57) Peleshanko, S.; Gunawidjaja, R.; Petrash, S.; Tsukruk, V. V. *Macromolecules* **2006**, *39*, 4756.
(58) Vogt, A. P.; Sumerlin, B. S. *Macromolecules* **2008**, *41*, 7368.
(59) Gao, H. F.; Min, K.; Matyjaszewski, K. *Macromolecules* **2009**, *42*, 8039.
(60) Gao, H. F.; Min, K.; Matyjaszewski, K. *J. Am. Chem. Soc.* **2007**, *129*, 11828.
(61) Gao, H. F.; Ohno, S.; Matyjaszewski, K. *J. Am. Chem. Soc.* **2006**, *128*, 15111.
(62) Baek, K. Y.; Kamigaito, M.; Sawamoto, M. *Macromolecules* **2001**, *34*, 7629.
(63) Baek, K. Y.; Kamigaito, M.; Sawamoto, M. *Macromolecules* **2002**, *35*, 1493.
(64) Gao, H. F.; Matyjaszewski, K. *Macromolecules* **2008**, *41*, 1118.
(65) Baek, K. Y.; Kamigaito, M.; Sawamoto, M. *Macromolecules* **2001**, *34*, 215.
(66) Hovestad, N. J.; van Koten, G.; Bon, S. A. F.; Haddleton, D. M. *Macromolecules* **2000**, *33*, 4048.
(67) Liu, J. Q.; Liu, H. Y.; Jia, Z. F.; Bulmus, V.; Davis, T. P. *Chem. Commun.* **2008**, 6582.
(68) Gao, H.; Matyjaszewski, K. *Macromolecules* **2006**, *39*, 4960.
(69) Whittaker, M. R.; Urbani, C. N.; Monteiro, M. J. *J. Am. Chem. Soc.* **2006**, *128*, 11360.
(70) Altintas, O.; Hizal, G.; Tunca, U. *J. Polym. Sci., Part A: Polym. Chem.* **2006**, *44*, 5699.
(71) Altintas, O.; Yankul, B.; Hizal, G.; Tunca, U. *J. Polym. Sci., Part A: Polym. Chem.* **2006**, *44*, 6458.
(72) Kasko, A. M.; Heintz, A. M.; Pugh, C. *Macromolecules* **1998**, *31*, 256.
(73) Hedrick, J. L.; Trollsås, M.; Hawker, C. J.; Atthoff, B.; Claesson, H.; Heise, A.; Miller, R. D. *Macromolecules* **1998**, *31*, 8691.

(74) Heise, A.; Hedrick, J. L.; Frank, C. W.; Miller, R. D. *J. Am. Chem. Soc.* **1999**, *121*, 8647.
(75) Angot, S.; Murthy, K. S.; Taton, D.; Gnanou, Y. *Macromolecules* **1998**, *31*, 7218.
(76) Haddleton, D. M.; Waterson, C. *Macromolecules* **1999**, *32*, 8732.
(77) Heise, A.; Diamanti, S.; Hedrick, J. L.; Franck, C. W.; Miller, R. D. *Macromolecules* **2001**, *34*, 3798.
(78) Huang, Y. K.; Liu, Q.; Zhou, X. D.; Perrier, S.; Zhao, Y. L. *Macromolecules* **2009**, *42*, 5509.
(79) Roovers, J. In *Star and Hyperbranched Polymers*; Mishra, M. K., Kobayashi, S., Eds.; Marcel Dekker: New York, 1999; pp 285−341.
(80) Douglas, J. F.; Roovers, J.; Freed, K. F. *Macromolecules* **1990**, *23*, 4168.
(81) Hou, T. T.; Zhang, P. P.; Zhou, X. D.; Cao, X. Q.; Zhao, Y. L. *Chem. Commun.* **2010**, *46*, 7397.
(82) Perrier, S.; Takolpuckdee, P.; Mars, C. A. *Macromolecules* **2005**, *38*, 6770.
(83) Chen, M.; Moad, G.; Rizzardo, E. *J. Polym. Sci., Part A: Polym. Chem.* **2009**, *47*, 6704.
(84) Cortez-Lemus, N. A.; Salgado-Rodríguez, R.; Licea-Claveríe, R. *J. Polym. Sci., Part A: Polym. Chem.* **2010**, *48*, 3033.
(85) Sasso, B.; Dobinson, M.; Hodge, P.; Wear, T. *Macromolecules* **2010**, *43*, 7453.